
FREE VIBRATION AND BUCKLING ANALYSIS OF TWO DIRECTIONAL FUNCTIONALLY GRADED BEAMS USING A FOUR-UNKNOWN SHEAR AND NORMAL DEFORMABLE BEAM THEORY

Armağan KARAMANLI *

Department of Mechatronics, Faculty of Engineering and Architecture, İstanbul Gelişim University,
34215, İstanbul, Turkey

ABSTRACT

This study presents the free vibration and buckling behavior of two directional (2D) functionally graded beams (FGBs) under arbitrary boundary conditions (BCs) for the first time. A four-known shear and normal deformation (Quasi-3D) theory where the axial and transverse displacements are assumed to be cubic and parabolic variation through the beam depth is employed based on the framework of the Ritz formulation. The equations of motion are derived from Lagrange's equations. The developed formulation is validated by solving a homogeneous beam problem and considering different aspect ratios and boundary conditions. The obtained numerical results in terms of dimensionless fundamental frequencies and dimensionless first critical buckling loads are compared with the results from previous studies for convergence studies. The material properties of the studied problems are assumed to vary along both longitudinal and thickness directions according to the power-law distribution. The axial, bending, shear and normal displacements are expressed in polynomial forms with the auxiliary functions which are necessary to satisfy the boundary conditions. The effects of shear deformation, thickness stretching, material distribution, aspect ratios and boundary conditions on the free vibration frequencies and critical buckling loads of the 2D-FGBs are investigated.

Keywords: 2D Functionally Graded Beam, Ritz Method, Quasi-3D Theory, Vibration, Buckling

1. INTRODUCTION

Functionally Graded Materials (FGMs) are a class of advanced composite materials whose material properties vary continuously in the desired directions. Since the use of this kind of materials avoids the stress concentration, cracking and interface problems through the layer interfaces in conventional composites, they have been using in many modern engineering applications such as military, aerospace, nuclear energy, biomedical, automotive, marine and civil engineering. Moreover, FGMs have lower transverse shear stresses and high resistance to temperature shocks. Due to their striking features, researchers have been developed the advanced theories and analysis methods to predict and to understand more precisely the behaviors of FGMs.

Since the significant shear deformation effects occur especially in thick/moderately thick conventional functionally graded beams (FGBs), three main theories that are first-order shear deformable beam theory (FSBT), higher-order shear deformable beam theory (HSBT) and shear and normal deformable beam theory (SNDBT) namely Quasi 3-D theory are popular among the researchers. The simplest model is the FSBT which does not satisfy the zero traction boundary conditions at the top and the bottom surfaces of the beam; however a shear correction factor is required [1-6]. This leads to the proposition of the HSBT theories which refined the distribution of the transverse shear stress; ultimately no shear correction factor is needed [7-19]. On the other hand, HSBT theories do not consider the normal strain effect which becomes very important and should be considered for thick conventional FGBs. Hence, quasi 3-D theories in which the shear and normal deformations taking into account are developed based on a higher order variation of both axial and transverse displacements [20-30].

The conventional FGBs (or 1D-FGBs) formed by changing material properties only in one direction may not satisfy required specifications such as the temperature and stress distributions in two or three direction for aerospace craft and shuttles [31]. In recent years, researchers have been devoted some studies about a new type FGB whose material properties varying in two or three directions to overcome this deficiency of the conventional FGBs. A methodology is presented for the simulation and optimization of the vibration response of bidirectional functionally graded beams based on the Element Free Galerkin method in [32]. The bending and thermal deformations of FGBs with various end conditions are investigated by using the state-space based differential quadrature method to obtain the semi-analytical elasticity solutions in [33]. The static and free vibration analysis two-directional FGBs are studied by presenting a symplectic elasticity solution in [34]. Free and forced vibration of Timoshenko two directional functionally graded beams under a moving load is investigated in [35] for the case that the material properties of the 2D-FGB vary exponentially through the length and height directions. Based on the power-law distribution of the material properties, the buckling of Timoshenko beams composed of two directional FGM is studied in [36]. The static behavior of the two directional FGBs by using various beam theories is presented in [37]. The fully coupled thermo-mechanical behavior of bi-directional functionally graded material (FGM) beam structures is studied via finite element method in [38]. An analytical solution for the static deformations of the bi-directional functionally graded thick circular beams is developed based on a new shear deformation theory with a logarithmic function in the postulated expression for the circumferential displacement in [39]. The flexure behavior of the two directional FG sandwich beams by using a quasi-3D theory and a meshless method is studied in [40]. Elasticity solutions of 2D-FG rotating annular and solid disks with variable thickness are presented in [41]. The vibration responses of 2D-FG Timoshenko beams excited by a moving concentrated load are investigated in [42]. In a very recent work by Hacıyev et al., the bending vibration of bi-directionally exponentially orthotropic plates resting on the Pasternak elastic foundation is studied based on the classical plate theory via Galerkin method [43].

It is clear from above discussions that the publications related to free vibration and buckling behavior of the two-directional FGBs are very limited according to the best of author knowledge. Moreover, there is no reported work on the dynamic and static analysis of the two directional FGBs based on a shear and normal deformation theory employing power-law material distribution in the problem domain. Since, thickness-stretching effect becomes very important especially for the thick two directional FGBs, a shear and normal deformation theory should be considered for this complicated problem with various end conditions, aspect ratios and gradation exponents. The main novelty of this paper is that the analytical solutions are presented for the free vibration and buckling behavior of the two directional FGBs based on a quasi-3D theory for the first time. The effects of shear deformation, thickness stretching, material distribution, aspect ratios and boundary conditions on the free vibration frequencies and critical buckling loads of the two directional functionally graded beams are discussed.

2. THEORY AND FORMULATION

2.1. Two Directional Functionally Graded Beams

Consider a two-directional functionally graded beam with its dimensions and coordinate as shown in Figure 1. The material properties vary both longitudinal and thickness directions. The origin of the coordinate system is at the midpoint of the beam. In this study, the rule of mixture is used to find the effective material properties at a point. The effective material properties of the beam, Young's modulus E and shear modulus G can be given by

$$\begin{aligned} E(x, z) &= E_1 V_1(x, z) + E_2 V_2(x, z) \\ G(x, z) &= G_1 V_1(x, z) + G_2 V_2(x, z) \\ \rho(x, z) &= \rho_1 V_1(x, z) + \rho_2 V_2(x, z) \end{aligned} \quad (1)$$

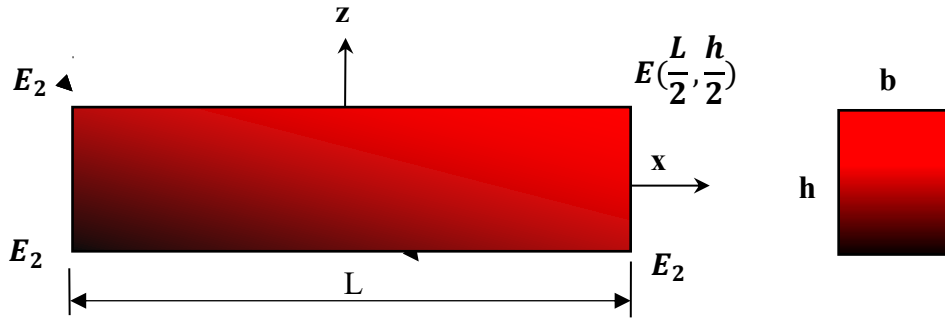


Figure 1. Geometry and coordinate of a two-directional FGB

According to the power law form, the volume fraction of the constitute 1 can be given by

$$V_1(x, z) = \left(\frac{1}{2} + \frac{x}{L}\right)^{p_x} \left(\frac{1}{2} + \frac{z}{h}\right)^{p_z} \quad (3)$$

where p_x and p_z are the gradation exponents (power-law index) which determine the material properties through the thickness (h) and length of the beam (L), respectively. When the p_x and p_z are set to zero then the beam becomes homogeneous. The effective material properties can be found by using the Eqs. (1), (2) and (3) as follows,

$$\begin{aligned} E(x, z) &= (E_1 - E_2) \left(\frac{1}{2} + \frac{x}{L}\right)^{p_x} \left(\frac{1}{2} + \frac{z}{h}\right)^{p_z} + E_2 \\ G(x, z) &= (G_1 - G_2) \left(\frac{1}{2} + \frac{x}{L}\right)^{p_x} \left(\frac{1}{2} + \frac{z}{h}\right)^{p_z} + G_2 \\ \rho(x, z) &= (\rho_1 - \rho_2) \left(\frac{1}{2} + \frac{x}{L}\right)^{p_x} \left(\frac{1}{2} + \frac{z}{h}\right)^{p_z} + \rho_2 \end{aligned} \quad (4)$$

2.2. Constitutive Equations

The axial and transverse displacements of a beam by using the present shear and normal deformation theory including both shear deformation and thickness stretching effects are given by

$$\begin{aligned} U(x, z, t) &= u(x, t) - z \frac{\partial w_b(x, t)}{\partial x} - \frac{4z^3}{3h^2} \frac{\partial w_s(x, t)}{\partial x} \\ &= u(x, t) - zw'_b(x, t) - f(z)w'_s(x, t) \end{aligned} \quad (5a)$$

$$\begin{aligned} W(x, z, t) &= w_b(x, t) + w_s(x, t) + \left(1 - \frac{4z^2}{h^2}\right)w_z(x, t) \\ &= w_b(x, t) + w_s(x, t) + g(z)w_z(x, t) \end{aligned} \quad (5b)$$

where u, w_b, w_s and w_z are four variables to be determined.

The only nonzero strains associated with the displacement field given in Eq. (5) can be written by:

$$\varepsilon_x = \frac{\partial U}{\partial x} = u' - zw''_b - f(z)w''_s \quad (6a)$$

$$\varepsilon_z = \frac{\partial W}{\partial z} = g'(z)w_z \quad (6b)$$

$$\gamma_{xz} = \frac{\partial W}{\partial x} + \frac{\partial U}{\partial z} = g(z)(w'_s + w'_z) \quad (6c)$$

The following linear elastic constitutive equation can be written by using the related stresses and strains based on the assumption of constant Poisson’s ratio for the sake of simplicity:

$$\begin{bmatrix} \sigma_x \\ \sigma_z \\ \sigma_{xz} \end{bmatrix} = \frac{E(x, z)}{1 - \nu^2} \begin{bmatrix} 1 & \nu & 0 \\ \nu & 1 & 0 \\ 0 & 0 & \frac{1 - \nu}{2} \end{bmatrix} \begin{bmatrix} \varepsilon_x \\ \varepsilon_z \\ \gamma_{xz} \end{bmatrix} \quad (7)$$

2.3. Variational Formulation

The strain energy of the beam including the energy associated with the shearing strain can be written as,

$$U = \frac{1}{2} \int_V (\sigma_x \varepsilon_x + \sigma_z \varepsilon_z + \sigma_{xz} \gamma_{xz}) dV \quad (8)$$

where V is the volume of the beam. Substituting Eqs. (6) and (7) into Eq. (8), the strain energy can be obtained as the form of:

$$U = \frac{1}{2} \int_V \frac{E(x, z)}{1 - \nu^2} \left[\varepsilon_x \varepsilon_x + 2\nu \varepsilon_x \varepsilon_z + \varepsilon_z \varepsilon_z + \frac{1 - \nu}{2} \gamma_{xz} \gamma_{xz} \right] dV \quad (9)$$

Where

$$\begin{aligned} \varepsilon_x \varepsilon_x &= \left(\frac{\partial u}{\partial x} \right)^2 + z^2 \left(\frac{\partial^2 w_b}{\partial x^2} \right)^2 + f^2 \left(\frac{\partial^2 w_s}{\partial x^2} \right)^2 - 2z \left(\frac{\partial u}{\partial x} \right) \left(\frac{\partial^2 w_b}{\partial x^2} \right) - 2f \left(\frac{\partial u}{\partial x} \right) \left(\frac{\partial^2 w_s}{\partial x^2} \right) \\ &\quad + 2fz \left(\frac{\partial^2 w_b}{\partial x^2} \right) \left(\frac{\partial^2 w_s}{\partial x^2} \right) \\ \varepsilon_x \varepsilon_z &= \left(\frac{dg}{dz} \right) \left(\frac{\partial u}{\partial x} \right) w_z - \left(\frac{dg}{dz} \right) z \left(\frac{\partial^2 w_b}{\partial x^2} \right) w_z - \left(\frac{dg}{dz} \right) f \left(\frac{\partial^2 w_s}{\partial x^2} \right) w_z \\ \varepsilon_z \varepsilon_z &= \left(\frac{dg}{dz} \right)^2 w_z^2 \\ \gamma_{xz} \gamma_{xz} &= g^2 \left(\frac{\partial w_s}{\partial x} \right)^2 + g^2 \left(\frac{\partial w_z}{\partial x} \right)^2 + 2g^2 \left(\frac{\partial w_s}{\partial x} \right) \left(\frac{\partial w_z}{\partial x} \right) \end{aligned} \quad (10)$$

It is useful to introduce the stiffness coefficients as follows:

$$(A, B, B_s, D, D_s, H, Z) = b \int_{-h/2}^{+h/2} \frac{(E_1 - E_2)}{1 - \nu^2} \left(\frac{1}{2} + \frac{z}{h} \right)^{p_z} (1, z, f, z^2, fz, f^2, g'^2) dz \quad (11a)$$

$$(A_1, B_1, B_{s1}, D_1, D_{s1}, H_1, Z_1) = b \int_{-h/2}^{+h/2} \frac{E_2}{1 - \nu^2} (1, z, f, z^2, fz, f^2, g'^2) dz \quad (11b)$$

$$A_s = b \int_{-h/2}^{+h/2} \frac{(E_1 - E_2)}{2(1 + \nu)} \left(\frac{1}{2} + \frac{z}{h} \right)^{p_z} g^2 dz \quad (11c)$$

$$A_{s1} = b \int_{-h/2}^{+h/2} \frac{E_2}{2(1 + \nu)} g^2 dz \quad (11d)$$

$$(X, Y, Y_s) = b \int_{-h/2}^{+h/2} \frac{(E_1 - E_2)v}{1 - v^2} \left(\frac{1}{2} + \frac{z}{h}\right)^{p_z} g'(1, z, f) dz \tag{11e}$$

$$(X_1, Y_1, Y_{s1}) = b \int_{-h/2}^{+h/2} \frac{E_2 v}{1 - v^2} g'(1, z, f) dz \tag{11f}$$

Using Eqs. 9 to 12, the strain energy can be written in the form of:

$$\begin{aligned} u = & \frac{1}{2} \int_{-L/2}^{L/2} \left[\left\{ A \left(\frac{1}{2} + \frac{x}{L}\right)^{p_x} + A_1 \right\} \left(\frac{\partial u}{\partial x}\right)^2 + \left\{ D \left(\frac{1}{2} + \frac{x}{L}\right)^{p_x} + D_1 \right\} \left(\frac{\partial^2 w_b}{\partial x^2}\right)^2 + \right. \\ & \left\{ H \left(\frac{1}{2} + \frac{x}{L}\right)^{p_x} + H_1 \right\} \left(\frac{\partial^2 w_s}{\partial x^2}\right)^2 + 2 \left\{ D_s \left(\frac{1}{2} + \frac{x}{L}\right)^{p_x} + D_{s1} \right\} \left(\frac{\partial^2 w_b}{\partial x^2}\right) \left(\frac{\partial^2 w_s}{\partial x^2}\right) - \\ & 2 \left\{ B \left(\frac{1}{2} + \frac{x}{L}\right)^{p_x} + B_1 \right\} \left(\frac{\partial u}{\partial x}\right) \left(\frac{\partial^2 w_b}{\partial x^2}\right) - 2 \left\{ B_s \left(\frac{1}{2} + \frac{x}{L}\right)^{p_x} + B_{s1} \right\} \left(\frac{\partial u}{\partial x}\right) \left(\frac{\partial^2 w_s}{\partial x^2}\right) + \\ & 2 \left\{ X \left(\frac{1}{2} + \frac{x}{L}\right)^{p_x} + X_1 \right\} \left(\frac{\partial u}{\partial x}\right) w_z - 2 \left\{ Y \left(\frac{1}{2} + \frac{x}{L}\right)^{p_x} + Y_1 \right\} \left(\frac{\partial^2 w_b}{\partial x^2}\right) w_z - \\ & 2 \left\{ Y_s \left(\frac{1}{2} + \frac{x}{L}\right)^{p_x} + Y_{s1} \right\} \left(\frac{\partial^2 w_s}{\partial x^2}\right) w_z + \left\{ Z \left(\frac{1}{2} + \frac{x}{L}\right)^{p_x} + Z_1 \right\} w_z^2 + \\ & \left. \left\{ A_s \left(\frac{1}{2} + \frac{x}{L}\right)^{p_x} + A_{s1} \right\} \left[\left(\frac{\partial w_s}{\partial x}\right)^2 + \left(\frac{\partial w_z}{\partial x}\right)^2 + 2 \left(\frac{\partial w_s}{\partial x}\right) \left(\frac{\partial w_z}{\partial x}\right) \right] \right] dx \tag{12} \end{aligned}$$

The potential energy of the axial N_0 and distributed $q(x)$ loads is given by

$$V = -\frac{1}{2} \int_{-L/2}^{L/2} N_0 \left\{ \left(\frac{\partial w_b}{\partial x}\right)^2 + 2 \frac{\partial w_b}{\partial x} \frac{\partial w_s}{\partial x} + \left(\frac{\partial w_s}{\partial x}\right)^2 \right\} dx - \int_0^L q(w_b + w_s) dx \tag{13}$$

The kinetic energy of present four-unknown shear and normal deformable beam theory can be obtained by using similar procedure as follows

$$\begin{aligned} K = & \frac{1}{2} \int_{-L/2}^{L/2} \left[\left\{ I_0 \left(\frac{1}{2} + \frac{x}{L}\right)^{p_x} + I_{00} \right\} \left\{ \left(\frac{\partial u}{\partial t}\right)^2 + \left(\frac{\partial w_b}{\partial t}\right)^2 + \left(\frac{\partial w_s}{\partial t}\right)^2 + 2 \left(\frac{\partial w_b}{\partial t}\right) \left(\frac{\partial w_s}{\partial t}\right) \right\} \right. \\ & - 2 \left\{ I_1 \left(\frac{1}{2} + \frac{x}{L}\right)^{p_x} + I_{11} \right\} \frac{\partial u}{\partial t} \frac{\partial^2 w_b}{\partial x \partial t} + \left\{ I_2 \left(\frac{1}{2} + \frac{x}{L}\right)^{p_x} + I_{22} \right\} \left(\frac{\partial^2 w_b}{\partial x \partial t}\right)^2 \\ & - 2 \left\{ J_1 \left(\frac{1}{2} + \frac{x}{L}\right)^{p_x} + J_{11} \right\} \frac{\partial u}{\partial t} \frac{\partial^2 w_s}{\partial x \partial t} \\ & + 2 \left\{ J_2 \left(\frac{1}{2} + \frac{x}{L}\right)^{p_x} + J_{22} \right\} \left\{ \left(\frac{\partial w_b}{\partial t}\right) \left(\frac{\partial w_z}{\partial t}\right) + \left(\frac{\partial w_s}{\partial t}\right) \left(\frac{\partial w_z}{\partial t}\right) \right\} \\ & + 2 \left\{ J_3 \left(\frac{1}{2} + \frac{x}{L}\right)^{p_x} + J_{33} \right\} \frac{\partial^2 w_b}{\partial x \partial t} \frac{\partial^2 w_s}{\partial x \partial t} + \left\{ K_1 \left(\frac{1}{2} + \frac{x}{L}\right)^{p_x} + K_{11} \right\} \left(\frac{\partial^2 w_s}{\partial x \partial t}\right)^2 \\ & \left. + \left\{ K_2 \left(\frac{1}{2} + \frac{x}{L}\right)^{p_x} + K_{22} \right\} \left(\frac{\partial w_z}{\partial t}\right)^2 \right] dx \tag{14} \end{aligned}$$

Here t is the time, and the inertial coefficients can be presented as

$$(I_0, I_1, I_2, J_1, J_2, J_3, K_1, K_2) = b \int_{-\frac{h}{2}}^{+\frac{h}{2}} (\rho_1 - \rho_2) \left(\frac{1}{2} + \frac{z}{h}\right)^{p_z} (1, z, z^2, f, g, fz, f^2, g^2) dz \quad (15a)$$

$$(I_{00}, I_{11}, I_{22}, J_{11}, J_{22}, J_{33}, K_{11}, K_{21}) = b \int_{-h/2}^{+h/2} \rho_2 (1, z, z^2, f, g, fz, f^2, g^2) dz \quad (15b)$$

The total potential energy (Π) can be obtained by using Eqs. (12), (13) and (14),

$$\Pi = \mathcal{U} + V - K$$

$$\begin{aligned} \Pi = \frac{1}{2} \int_{-L/2}^{L/2} & \left[\left\{ A \left(\frac{1}{2} + \frac{x}{L} \right)^{p_x} + A_1 \right\} \left(\frac{\partial u}{\partial x} \right)^2 + \left\{ D \left(\frac{1}{2} + \frac{x}{L} \right)^{p_x} + D_1 \right\} \left(\frac{\partial^2 w_b}{\partial x^2} \right)^2 \right. \\ & + \left\{ H \left(\frac{1}{2} + \frac{x}{L} \right)^{p_x} + H_1 \right\} \left(\frac{d^2 w_s}{dx^2} \right)^2 + 2 \left\{ D_s \left(\frac{1}{2} + \frac{x}{L} \right)^{p_x} + D_{s1} \right\} \left(\frac{\partial^2 w_b}{\partial x^2} \right) \left(\frac{\partial^2 w_s}{\partial x^2} \right) \\ & - 2 \left\{ B \left(\frac{1}{2} + \frac{x}{L} \right)^{p_x} + B_1 \right\} \left(\frac{\partial u}{\partial x} \right) \left(\frac{\partial^2 w_b}{\partial x^2} \right) - 2 \left\{ B_s \left(\frac{1}{2} + \frac{x}{L} \right)^{p_x} + B_{s1} \right\} \left(\frac{\partial u}{\partial x} \right) \left(\frac{\partial^2 w_s}{\partial x^2} \right) \\ & + 2 \left\{ X \left(\frac{1}{2} + \frac{x}{L} \right)^{p_x} + X_1 \right\} \left(\frac{\partial u}{\partial x} \right) w_z - 2 \left\{ Y \left(\frac{1}{2} + \frac{x}{L} \right)^{p_x} + Y_1 \right\} \left(\frac{\partial^2 w_b}{\partial x^2} \right) w_z \\ & - 2 \left\{ Y_s \left(\frac{1}{2} + \frac{x}{L} \right)^{p_x} + Y_{s1} \right\} \left(\frac{\partial^2 w_s}{\partial x^2} \right) w_z + \left\{ Z \left(\frac{1}{2} + \frac{x}{L} \right)^{p_x} + Z_1 \right\} w_z^2 \\ & + \left\{ A_s \left(\frac{1}{2} + \frac{x}{L} \right)^{p_x} + A_{s1} \right\} \left\{ \left(\frac{\partial w_s}{\partial x} \right)^2 + \left(\frac{\partial w_z}{\partial x} \right)^2 + 2 \left(\frac{\partial w_s}{\partial x} \right) \left(\frac{\partial w_z}{\partial x} \right) \right\} \\ & - \left\{ I_0 \left(\frac{1}{2} + \frac{x}{L} \right)^{p_x} + I_{00} \right\} \left\{ \left(\frac{\partial u}{\partial t} \right)^2 + \left(\frac{\partial w_b}{\partial t} \right)^2 + \left(\frac{\partial w_s}{\partial t} \right)^2 + 2 \left(\frac{\partial w_b}{\partial t} \right) \left(\frac{\partial w_s}{\partial t} \right) \right\} \\ & + 2 \left\{ I_1 \left(\frac{1}{2} + \frac{x}{L} \right)^{p_x} + I_{11} \right\} \frac{\partial u}{\partial t} \frac{\partial^2 w_b}{\partial x \partial t} - \left\{ I_2 \left(\frac{1}{2} + \frac{x}{L} \right)^{p_x} + I_{22} \right\} \left(\frac{\partial^2 w_b}{\partial x \partial t} \right)^2 \\ & + 2 \left\{ J_1 \left(\frac{1}{2} + \frac{x}{L} \right)^{p_x} + J_{11} \right\} \frac{\partial u}{\partial t} \frac{\partial^2 w_s}{\partial x \partial t} - 2 \left\{ J_2 \left(\frac{1}{2} + \frac{x}{L} \right)^{p_x} + J_{22} \right\} \left\{ \left(\frac{\partial w_b}{\partial t} \right) \left(\frac{\partial w_z}{\partial t} \right) + \left(\frac{\partial w_s}{\partial t} \right) \left(\frac{\partial w_z}{\partial t} \right) \right\} \\ & - 2 \left\{ J_3 \left(\frac{1}{2} + \frac{x}{L} \right)^{p_x} + J_{33} \right\} \frac{\partial^2 w_b}{\partial x \partial t} \frac{\partial^2 w_s}{\partial x \partial t} - \left\{ K_1 \left(\frac{1}{2} + \frac{x}{L} \right)^{p_x} + K_{11} \right\} \left(\frac{\partial^2 w_s}{\partial x \partial t} \right)^2 \\ & \left. - \left\{ K_2 \left(\frac{1}{2} + \frac{x}{L} \right)^{p_x} + K_{22} \right\} \left(\frac{\partial w_z}{\partial t} \right)^2 - N_0 \left\{ \left(\frac{\partial w_b}{\partial x} \right)^2 + 2 \frac{\partial w_b}{\partial x} \frac{\partial w_s}{\partial x} + \left(\frac{\partial w_s}{\partial x} \right)^2 \right\} - 2q(w_b + w_s) \right] dx \quad (15) \end{aligned}$$

2.4. Solution Procedure

It is known that Hamilton's principle can be expressed as Lagrange equations when the functions of infinite dimensions can be expressed in terms of generalized coordinates. Therefore, the displacement functions $u(x)$, $w_b(x)$, $w_s(x)$ and $w_z(x)$ are presented by the following polynomial series which are satisfy the kinematic boundary conditions given in Table 1,

$$u(x) = \sum_{j=1}^m A_j e^{i\omega t} \theta_j(x), \quad \theta_j(x) = \left(x + \frac{L}{2}\right)^{p_u} \left(x - \frac{L}{2}\right)^{q_u} x^{j-1} \quad (16a)$$

$$w_b(x) = \sum_{j=1}^m B_j e^{i\omega t} \varphi_j(x), \quad \varphi_j(x) = \left(x + \frac{L}{2}\right)^{p_{w_b}} \left(x - \frac{L}{2}\right)^{q_{w_b}} x^{j-1} \quad (16b)$$

$$w_s(x) = \sum_{j=1}^m C_j e^{i\omega t} \zeta_j(x), \quad \zeta_j(x) = \left(x + \frac{L}{2}\right)^{p_{w_s}} \left(x - \frac{L}{2}\right)^{q_{w_s}} x^{j-1} \quad (16c)$$

$$w_z(x) = \sum_{j=1}^m D_j e^{i\omega t} \psi_j(x), \quad \psi_j(x) = \left(x + \frac{L}{2}\right)^{p_{w_z}} \left(x - \frac{L}{2}\right)^{q_{w_z}} x^{j-1} \quad (16d)$$

where A_j, B_j, C_j and D_j are unknown values to be determined, ω is the natural frequency of the beam, $i = \sqrt{-1}$ is the complex number, $\theta_j(x), \varphi_j(x), \zeta_j(x)$ and $\psi_j(x)$ are the shape functions which are proposed for the boundary conditions (BCs) to be studied within this paper, p_ξ and q_ξ ($\xi = u, w_b, w_s, w_z$) are the boundary exponents of the auxiliary functions related with the boundary conditions given in Table 2. It has to be mentioned that the shape functions which do not satisfy the boundary conditions may cause slow convergence rates and numerical instabilities.

Table 1. Kinematic boundary conditions used for the numerical computations.

BC	$x=-L/2$	$x=L/2$
SS	$u = 0, w_b = 0, w_s = 0, w_z = 0$	$w_b = 0, w_s = 0, w_z = 0$
CS	$u = 0, w_b = 0, w_s = 0, w_z = 0, w_b' = 0, w_s' = 0$	$w_b = 0, w_s = 0, w_z = 0$
CC	$u = 0, w_b = 0, w_s = 0, w_z = 0, w_b' = 0, w_s' = 0$	$u = 0, w_b = 0, w_s = 0, w_z = 0, w_b' = 0, w_s' = 0$
CF	$u = 0, w_b = 0, w_s = 0, w_z = 0, w_b' = 0, w_s' = 0$	

Table 2. Boundary exponents for various boundary conditions.

BC	Left end				Right end			
	p_u	p_{w_b}	p_{w_s}	p_{w_z}	q_u	q_{w_b}	q_{w_s}	q_{w_z}
SS	1	1	1	1	0	1	1	1
CS	1	2	2	1	0	1	1	1
CC	1	2	2	1	1	2	2	1
CF	1	2	2	1	0	0	0	0

The governing equations of motion for free vibration analysis can be obtained by substituting Eq. (16) into Eq. (15) and using Lagrange equations

$$\frac{\partial \Pi}{\partial q_j} - \frac{\partial}{\partial t} \left(\frac{\partial \Pi}{\partial \dot{q}_j} \right) = 0 \quad (17)$$

with q_j representing the values of $(A_j, B_j, C_j$ and $D_j)$, that leads to

$$\left(\begin{bmatrix} [K_{11}] & [K_{12}] & [K_{13}] & [K_{14}] \\ [K_{12}]^T & [K_{22}] & [K_{23}] & [K_{24}] \\ [K_{13}]^T & [K_{23}]^T & [K_{33}] & [K_{34}] \\ [K_{14}]^T & [K_{24}]^T & [K_{34}]^T & [K_{44}] \end{bmatrix} - \omega^2 \begin{bmatrix} [M_{11}] & [M_{12}] & [M_{13}] & [M_{14}] \\ [M_{12}]^T & [M_{22}] & [M_{23}] & [M_{24}] \\ [M_{13}]^T & [M_{23}]^T & [M_{33}] & [M_{34}] \\ [M_{14}]^T & [M_{24}]^T & [M_{34}]^T & [M_{44}] \end{bmatrix} \right) \begin{Bmatrix} \{A\} \\ \{B\} \\ \{C\} \\ \{D\} \end{Bmatrix} = \begin{Bmatrix} \{0\} \\ \{0\} \\ \{0\} \\ \{0\} \end{Bmatrix} \quad (18)$$

where $[K_{kl}]$ are the stiffness matrices and $[M_{kl}]$ are the mass matrices. It should be noted that the stiffness and mass matrices are symmetric and in size $m \times m$.

The components of the stiffness and mass matrices are given by:

$$\begin{aligned}
 K_{11}(i, j) &= \int_{-L/2}^{L/2} \left[A \left(\frac{1}{2} + \frac{x}{L} \right)^{p_x} + A_1 \right] \theta_{i,x} \theta_{j,x} dx, \\
 K_{12}(i, j) &= - \int_{-L/2}^{L/2} \left[B \left(\frac{1}{2} + \frac{x}{L} \right)^{p_x} + B_1 \right] \theta_{i,x} \varphi_{j,xx} dx, \\
 K_{13}(i, j) &= - \int_{-L/2}^{L/2} \left[B_s \left(\frac{1}{2} + \frac{x}{L} \right)^{p_x} + B_{s1} \right] \theta_{i,x} \zeta_{j,xx} dx, \\
 K_{14}(i, j) &= \int_{-L/2}^{L/2} \left[X \left(\frac{1}{2} + \frac{x}{L} \right)^{p_x} + X_1 \right] \theta_{i,x} \psi_j dx, \\
 K_{22}(i, j) &= \int_{-L/2}^{L/2} \left[D \left(\frac{1}{2} + \frac{x}{L} \right)^{p_x} + D_1 \right] \varphi_{i,xx} \varphi_{j,xx} dx - N_0 \int_{-L/2}^{L/2} \varphi_{i,x} \varphi_{j,x} dx \\
 K_{23}(i, j) &= \int_{-L/2}^{L/2} \left[D_s \left(\frac{1}{2} + \frac{x}{L} \right)^{p_x} + D_{s1} \right] \varphi_{i,xx} \zeta_{j,xx} dx - N_0 \int_{-L/2}^{L/2} \varphi_{i,x} \zeta_{j,x} dx \\
 K_{24}(i, j) &= - \int_{-L/2}^{L/2} \left[Y \left(\frac{1}{2} + \frac{x}{L} \right)^{p_x} + Y_1 \right] \varphi_{i,xx} \psi_j dx \\
 K_{33}(i, j) &= \int_{-L/2}^{L/2} \left[H \left(\frac{1}{2} + \frac{x}{L} \right)^{p_x} + H_1 \right] \zeta_{i,xx} \zeta_{j,xx} dx + \int_{-L/2}^{L/2} \left[A_s \left(\frac{1}{2} + \frac{x}{L} \right)^{p_x} + A_{s1} \right] \zeta_{i,x} \zeta_{j,x} dx \\
 &\quad - N_0 \int_{-L/2}^{L/2} \zeta_{i,x} \zeta_{j,x} dx - \int_{-L/2}^{L/2} q(x) \zeta_i \zeta_j dx \\
 K_{34}(i, j) &= - \int_{-L/2}^{L/2} \left[Y_s \left(\frac{1}{2} + \frac{x}{L} \right)^{p_x} + Y_{s1} \right] \zeta_{i,xx} \psi_j dx + \int_{-L/2}^{L/2} \left[A_s \left(\frac{1}{2} + \frac{x}{L} \right)^{p_x} + A_{s1} \right] \zeta_{i,x} \psi_{j,x} dx \\
 K_{44}(i, j) &= \int_{-L/2}^{L/2} \left[Z \left(\frac{1}{2} + \frac{x}{L} \right)^{p_x} + Z_1 \right] \psi_i \psi_j dx + \int_{-L/2}^{L/2} \left[A_s \left(\frac{1}{2} + \frac{x}{L} \right)^{p_x} + A_{s1} \right] \psi_{i,x} \psi_{j,x} dx \\
 M_{11}(i, j) &= \int_{-L/2}^{L/2} \left[I_0 \left(\frac{1}{2} + \frac{x}{L} \right)^{p_x} + I_{00} \right] \theta_i \theta_j dx, \\
 M_{12}(i, j) &= - \int_{-L/2}^{L/2} \left[I_1 \left(\frac{1}{2} + \frac{x}{L} \right)^{p_x} + I_{11} \right] \theta_i \varphi_{j,x} dx, \\
 M_{13}(i, j) &= - \int_{-L/2}^{L/2} \left[J_1 \left(\frac{1}{2} + \frac{x}{L} \right)^{p_x} + J_{11} \right] \theta_i \zeta_{j,x} dx \\
 M_{14}(i, j) &= 0
 \end{aligned}$$

$$\begin{aligned}
 M_{22}(i, j) &= \int_{-L/2}^{L/2} \left[I_0 \left(\frac{1}{2} + \frac{x}{L} \right)^{p_x} + I_{00} \right] \varphi_i \varphi_j dx + \int_{-L/2}^{L/2} \left[I_2 \left(\frac{1}{2} + \frac{x}{L} \right)^{p_x} + I_{22} \right] \varphi_{i,x} \varphi_{j,x} dx \\
 M_{23}(i, j) &= \int_{-L/2}^{L/2} \left[I_0 \left(\frac{1}{2} + \frac{x}{L} \right)^{p_x} + I_{00} \right] \varphi_i \zeta_j dx + \int_{-L/2}^{L/2} \left[J_3 \left(\frac{1}{2} + \frac{x}{L} \right)^{p_x} + J_{33} \right] \varphi_{i,x} \zeta_{j,x} dx \\
 M_{24}(i, j) &= \int_{-L/2}^{L/2} \left[J_2 \left(\frac{1}{2} + \frac{x}{L} \right)^{p_x} + J_{22} \right] \varphi_i \psi_j dx \\
 M_{33}(i, j) &= \int_{-L/2}^{L/2} \left[I_0 \left(\frac{1}{2} + \frac{x}{L} \right)^{p_x} + I_{00} \right] \zeta_i \zeta_j dx + \int_{-L/2}^{L/2} \left[K_1 \left(\frac{1}{2} + \frac{x}{L} \right)^{p_x} + K_{11} \right] \zeta_{i,x} \zeta_{j,x} dx \\
 M_{34}(i, j) &= \int_{-L/2}^{L/2} \left[J_2 \left(\frac{1}{2} + \frac{x}{L} \right)^{p_x} + J_{22} \right] \zeta_i \psi_j dx \\
 M_{44}(i, j) &= \int_{-L/2}^{L/2} \left[K_2 \left(\frac{1}{2} + \frac{x}{L} \right)^{p_x} + K_{22} \right] \psi_i \psi_j dx \quad i, j = 1, 2, 3, \dots, m \quad (19)
 \end{aligned}$$

The free vibration and buckling behavior of the two directional FGBs can be investigated by using Eqs. (18) and (19).

3. NUMERICAL RESULTS

In this section a number of numerical examples are presented to discuss the effects of gradient indexes (or material composition), aspect ratios and boundary conditions on the critical buckling loads and natural frequencies of the two directional FGBs using a quasi-3D shear deformation theory. It is assumed that the Poisson’s ratio is constant and the material properties vary along both longitudinal and thickness directions according to the power-law distribution. Two different aspect ratios (L/h) 5 and 20 are considered with arbitrary boundary conditions, namely simply supported-simply supported (SS), clamped-simply supported (CS), clamped-clamped (CC) and clamped-free (CF).

The material properties of the two constitutes are given as

Ceramic (Al_2O_3) : $E_1 = 380GPa, \nu_1 = 0.3$ and $\rho_1 = 3960 kg/m^3$

Metal (*Aluminium*) : $E_2 = 70GPa, \nu_2 = 0.3$ and $\rho_2 = 2702 kg/m^3$

The following non-dimensional quantities are used for the representation of the results;

The dimensionless buckling load (\bar{N}_{cr})

$$\bar{N}_{cr} = \frac{12N_{cr}L^2}{E_2bh^3} \quad (20)$$

The dimensionless frequency (λ)

$$\lambda = \frac{\omega L^2}{h} \sqrt{\frac{\rho_2}{E_2}} \quad (21)$$

Table 3. Verification and convergence studies, dimensionless fundamental frequency (λ) of homogeneous beams with respect to various boundary conditions and aspect ratio change.

L/h	Reference	Boundary Condition			
		SS	CC	CF	
5	HBT [23]	5.1528	10.0726	1.8953	
	Quasi-3D [24]	5.1618	10.1851	1.9055	
	Quasi-3D [25]	5.1620	10.1790	1.9053	
	Present	2 terms	5.7158	10.5992	1.9477
		4 terms	5.1631	10.3276	1.9172
		6 terms	5.1616	10.2488	1.9107
		8 terms	5.1616	10.2064	1.9078
		10 terms	5.1616	10.1835	1.9061
12 terms	5.1616	10.1759	1.9053		
14 terms	5.1616	10.1748	1.9051		
20	HBT [23]	5.4603	12.2243	1.9496	
	Quasi-3D [24]	5.4610	12.2660	1.9527	
	Quasi-3D [25]	5.4611	12.2756	1.9530	
	Present	2 terms	6.1034	12.7736	1.9959
		4 terms	5.4627	12.3896	1.9647
		6 terms	5.4610	12.3218	1.9577
		8 terms	5.4610	12.2930	1.9549
		10 terms	5.4610	12.2794	1.9537
12 terms	5.4610	12.2721	1.9531		
14 terms	5.4610	12.2676	1.9527		

Firstly, the numerical computations are performed for the convergence analysis to make comparison studies along with the solutions from previous studies [18-24-29]. The convergence and verification studies are carried out by employing different number of terms in the displacement functions ($m=2, 4, 6, 8, 10, 12$ and 14) and different aspect ratios ($L/h=5$ and 20). The computed results are presented in terms of dimensionless fundamental frequencies and dimensionless critical buckling loads of a homogenous beam considering various boundary conditions, namely SS, CC and CF. The present results based on the dimensionless fundamental frequencies of the homogenous beams agree well with those from the previous studies [18-24-29]. It can be seen that for the free vibration analysis of SS beams, the responses converge quickly, when the number of terms in polynomial expansion is set to 6 as given in Table 3. However, the agreed results are obtained for CC and CF boundary conditions by employing 10 terms in polynomial expansion as it is seen in Table 3. It is clear that the dimensionless fundamental frequencies obtained based on the Quasi-3D theories are a bit higher than the ones based on the HBT. For the sake of accuracy, 12 terms in the polynomial expansion is employed for the extensive free vibration analysis of two directional FGBs.

Table 4. Verification and convergence studies, dimensionless critical buckling loads (\bar{N}_{cr}) of homogeneous beams with respect to various boundary conditions and aspect ratio change.

L/h	Reference	Boundary Condition			
		SS	CC	CF	
5	HBT [23]	48.5964	152.1588	13.0595	
	Quasi-3D [24]	49.5906	160.2780	13.1224	
	Quasi-3D [25]	49.5970	160.3064	13.1138	
	Present	2 terms	59.9462	169.2615	13.6065
		4 terms	49.6171	160.5097	13.2304
		6 terms	49.5906	160.3503	13.1653
		8 terms	49.5906	160.3145	13.1289
		10 terms	49.5906	160.2839	13.1178
12 terms	49.5906	160.2679	13.1140		
14 terms	49.5906	160.2662	13.1115		
20	HBT [23]	53.2364	208.9515	13.3730	
	Quasi-3D [24]	53.3145	210.7420	13.3981	
	Quasi-3D [25]	53.3175	210.7774	13.3993	
	Present	2 terms	65.7932	239.9515	13.8748
		4 terms	53.3455	212.3740	13.4792
		6 terms	53.3145	211.4672	13.4313
		8 terms	53.3145	211.0324	13.4126
		10 terms	53.3145	210.8367	13.4040
12 terms	53.3145	210.7416	13.3996		
14 terms	53.3145	210.6946	13.3971		

Regarding to the numerical results for the dimensionless critical buckling loads given in Table 4, it is clear that for SS beams, the computed first critical buckling loads show excellent agreement when the number of terms in the displacement functions is set to 6. Agreed results are obtained as the number of terms in the displacement functions is set to 10 for CC and CF beams. The computed results based on the present Quasi – 3D theory is higher than the ones obtained by the HBT theory. The extensive studies based on the buckling behavior of two directional FGBs are performed by employing 12 terms in the displacement functions. In Tables 5-8, the first three dimensionless frequencies of the 2D-FGBs with SS, CS, CC and CF boundary conditions are presented for two different aspect ratios ($L/h=5$ and 20) and various gradient indexes in both directions (p_z and p_x). It is observed that that the first three dimensionless frequencies decrease for all type of end conditions except CF beams while the gradient indexes increase. For CF beams with $p_x \geq 2$, the dimensionless fundamental frequencies increase as the gradient index in the z direction increases for the studied aspect ratios. Moreover, the second dimensionless frequencies of CF beams with $p_x = 10$ increase as the gradient index in the z direction increases. And finally, the third dimensionless frequencies of CF beams with $p_x \geq 5$ increase as the gradient index in the z direction increases only for the aspect ratio 5. It is expected that the frequencies have to decrease since the Young’s modulus, ultimately the rigidity of the beam decreases with the increase of the gradient indexes. However, the mass is not constant and decreased by the material gradient indexes. It is very well known in vibration theory and should be noted that the frequency is inversely proportional with the mass of the beam. It is clear that the effect of the mass on the first three dimensionless frequencies of the SS, CS and CC beams is a bit more dominant than the effect of the Young’s modulus.

Table 5. The first three dimensionless frequencies of SS two directional FGBs with respect to gradient index and aspect ratio change.

λ	p_x	p_z											
		$L/h=5$						$L/h=20$					
		0	0.5	1	2	5	10	0	0.5	1	2	5	10
λ_1	0	5.1616	4.4236	4.0073	3.6434	3.4126	3.2898	5.4610	4.6658	4.2345	3.8763	3.6822	3.5589
	0.5	4.6312	4.0223	3.7065	3.4470	3.2724	3.1586	4.9210	4.2586	3.9284	3.6711	3.5172	3.3958
	1	4.1791	3.7055	3.4744	3.2888	3.1504	3.0499	4.4310	3.9173	3.6762	3.4936	3.3703	3.2634
	2	3.5772	3.3007	3.1727	3.0685	2.9758	2.9045	3.7660	3.4718	3.3414	3.2435	3.1642	3.0912
	5	2.9643	2.8841	2.8468	2.8132	2.7758	2.7488	3.1030	3.0222	2.9881	2.9620	2.9360	2.9118
	10	2.7726	2.7493	2.7373	2.7248	2.7092	2.6997	2.9071	2.8860	2.8773	2.8705	2.8630	2.8564
λ_2	0	15.8455	13.9581	12.5700	11.1032	9.8030	9.2152	21.5835	18.4530	16.7400	15.3000	14.4865	13.9937
	0.5	12.0062	11.1381	10.5612	9.9133	9.1984	8.8160	19.2395	16.6946	15.4215	14.4158	13.7879	13.3164
	1	10.0770	9.7108	9.4647	9.1619	8.7745	8.5557	17.3484	15.3895	14.4511	13.7186	13.2184	12.8205
	2	8.6965	8.6391	8.5833	8.5011	8.3895	8.3277	15.1628	13.9183	13.3337	12.8787	12.5453	12.2684
	5	8.0148	8.0946	8.1297	8.1630	8.1983	8.2155	12.9496	12.4183	12.1807	11.9976	11.8380	11.6945
	10	7.9888	8.0690	8.1092	8.1497	8.1913	8.2105	11.8844	11.6838	11.5980	11.5304	11.4606	11.3984
λ_3	0	17.9716	15.7982	14.6193	13.3673	12.0190	11.2896	47.6417	40.7450	36.9057	33.6081	31.6248	30.5486
	0.5	15.8647	13.9906	12.9844	12.0412	11.1769	10.7077	42.2638	36.7311	33.9375	31.6950	30.2317	29.2003
	1	14.3020	12.8353	12.0631	11.3601	10.7352	10.3812	38.0997	33.8924	31.8456	30.2096	29.0457	28.1740
	2	12.5555	11.6170	11.1376	10.7059	10.2974	10.0454	33.4581	30.7594	29.4675	28.4350	27.6526	27.0403
	5	10.7851	10.3884	10.1936	10.0111	9.8061	9.6698	28.8297	27.5972	27.0195	26.5604	26.1796	25.8618
	10	9.9806	9.8194	9.7366	9.6493	9.5379	9.4692	26.6522	26.0903	25.8388	25.6381	25.4434	25.2749

Table 6. The first three dimensionless frequencies of CS two directional FGBs with respect to gradient index and aspect ratio change.

λ	p_x	p_z											
		$L/h=5$						$L/h=20$					
		0	0.5	1	2	5	10	0	0.5	1	2	5	10
λ_1	0	7.6552	6.6074	6.0067	5.4570	5.0342	4.8103	8.5094	7.2741	6.6023	6.0420	5.7312	5.5356
	0.5	6.3567	5.6592	5.2849	4.9519	4.6758	4.5131	6.9971	6.1958	5.7964	5.4853	5.2971	5.1431
	1	5.7603	5.2358	4.9598	4.7156	4.5065	4.3792	6.3149	5.7242	5.4385	5.2207	5.0816	4.9588
	2	5.1928	4.8393	4.6597	4.4986	4.3452	4.2475	5.6590	5.2746	5.0979	4.9655	4.8672	4.7747
	5	4.5065	4.3661	4.2938	4.2207	4.1348	4.0829	4.8831	4.7442	4.6844	4.6385	4.5939	4.5523
	10	4.1951	4.1439	4.1134	4.0798	4.0351	4.0112	4.5636	4.5215	4.5037	4.4893	4.4735	4.4597
λ_2	0	15.8455	14.2559	13.2040	11.9300	10.3600	9.4973	27.1362	23.2313	21.0898	19.2763	18.2034	17.5525
	0.5	12.0062	11.1856	10.6542	10.0210	9.2537	8.8375	23.2137	20.3810	18.9464	17.7948	17.0570	16.5150
	1	10.0770	9.7128	9.4677	9.1637	8.7748	8.5559	21.1411	18.9382	17.8570	17.0011	16.4223	15.9724
	2	8.6965	8.6420	8.5906	8.5134	8.4010	8.3348	18.9078	17.4079	16.6928	16.1306	15.7215	15.3883
	5	8.0148	8.0962	8.1333	8.1683	8.2026	8.2180	16.3260	15.6444	15.3353	15.0967	14.8958	14.7165
	10	7.9888	8.0691	8.1095	8.1501	8.1916	8.2107	15.0092	14.7358	14.6186	14.5273	14.4362	14.3532
λ_3	0	21.0092	18.3303	16.6967	15.0492	13.4913	12.7572	55.3449	47.4742	43.1077	39.3361	36.9305	35.5329
	0.5	17.9388	15.9748	14.8466	13.7410	12.7143	12.2179	47.9082	41.9833	38.9482	36.4552	34.7599	33.6082
	1	16.2359	14.7230	13.8783	13.0664	12.3229	11.9458	40.3079	38.7665	36.6664	34.8267	33.5090	32.5477
	2	14.4376	13.4283	12.8877	12.3816	11.9126	11.6505	34.7862	34.5556	34.1544	32.9763	32.0645	31.3617
	5	12.4407	12.0153	11.8041	11.6113	11.4112	11.2778	32.0591	32.0686	31.4021	30.8587	30.4045	30.0354
	10	11.5509	11.3841	11.3031	11.2247	11.1294	11.0649	31.0525	30.3768	30.0691	29.8196	29.5774	29.3748

On the other hand, depending on the gradient index in the x direction, mode numbers and aspect ratios, the vibration behavior of the 2D- FGBs with CF boundary condition is significantly affected with the variation of the mass and Young’s modulus. It is clear that the reduction in the dimensionless free vibration frequencies because of the gradient index variation in the x direction is more than the gradient index variation in the z direction for all type of end conditions. The highest free vibration frequencies for 2D-FGBs are obtained as the CC boundary condition is employed. As it is expected, the lowest frequencies are observed for CF beams followed by SS and CS beams.

Table 7. The first three dimensionless frequencies of CC two directional FGBs with respect to gradient index and aspect ratio change.

λ	p_x	p_z											
		$L/h=5$						$L/h=20$					
		0	0.5	1	2	5	10	0	0.5	1	2	5	10
λ_1	0	10.1759	8.8542	8.0672	7.2947	6.5887	6.2416	12.2721	10.4992	9.5300	8.7146	8.2446	7.9552
	0.5	8.6837	7.7335	7.1984	6.6815	6.1950	5.9474	10.4425	9.1841	8.5464	8.0341	7.7086	7.4680
	1	8.0146	7.2454	6.8189	6.4068	6.0187	5.8206	9.6508	8.6350	8.1285	7.7202	7.4470	7.2446
	2	7.4211	6.8138	6.4827	6.1621	5.8589	5.7035	8.9312	8.1392	7.7478	7.4274	7.1994	7.0345
	5	6.7044	6.3084	6.0929	5.8831	5.6831	5.5777	8.1208	7.5925	7.3283	7.1056	6.9363	6.8177
	10	6.2354	5.9793	5.8418	5.7098	5.5829	5.5105	7.6339	7.2699	7.0859	6.9279	6.8005	6.7087
λ_2	0	24.3589	21.3564	19.4838	17.5186	15.5157	14.5968	33.2845	28.5171	25.8895	23.6467	22.2759	21.4594
	0.5	21.1061	18.8226	17.4750	16.0908	14.6829	14.0309	28.7587	25.2140	23.4044	21.9294	20.9462	20.2556
	1	19.2354	17.4322	16.3953	15.3416	14.2693	13.7605	26.3398	23.5295	22.1316	20.9986	20.2035	19.6256
	2	17.2189	15.9694	15.2693	14.5617	13.8333	13.4745	23.7650	21.7720	20.7950	19.9962	19.4007	18.9640
	5	15.1832	14.4989	14.1212	13.7415	13.3534	13.1571	21.0582	19.9316	19.3703	18.8965	18.5278	18.2667
	10	14.3429	13.8876	13.6351	13.3837	13.1361	13.0123	19.8630	19.1102	18.7254	18.3937	18.1345	17.9567
λ_3	0	31.6911	28.5167	26.4184	23.8732	20.7275	18.9992	63.3236	54.4023	49.4097	45.0337	42.0880	40.4225
	0.5	26.9491	24.5911	23.0946	21.3277	19.2155	18.0898	55.0410	48.2705	44.7633	41.8264	39.7191	38.3415
	1	24.8720	22.9287	21.7150	20.2962	18.6227	17.7392	50.1770	44.8691	42.2028	39.9891	38.3169	37.1679
	2	23.2602	21.6318	20.6357	19.4897	18.1606	17.4672	44.8669	41.2414	39.4503	37.9492	36.7350	35.8824
	5	20.8850	19.8707	19.2443	18.5099	17.6318	17.1623	39.4386	37.5307	36.5711	35.7345	35.0129	34.5259
	10	19.0593	18.5083	18.1557	17.7273	17.1985	16.9091	37.1394	35.9281	35.2980	34.7303	34.2408	33.9319

Table 8. The first three dimensionless frequencies of CF two directional FGBs with respect to gradient index and aspect ratio change.

λ	p_x	p_z											
		$L/h=5$						$L/h=20$					
		0	0.5	1	2	5	10	0	0.5	1	2	5	10
λ_1	0	1.9053	1.6311	1.4803	1.3523	1.2762	1.2308	1.9531	1.6684	1.5141	1.3863	1.3176	1.2737
	0.5	1.3346	1.2291	1.1802	1.1455	1.1225	1.0972	1.3585	1.2510	1.2030	1.1715	1.1542	1.1299
	1	1.0953	1.0646	1.0534	1.0491	1.0474	1.0378	1.1137	1.0834	1.0736	1.0722	1.0746	1.0660
	2	0.9526	0.9640	0.9724	0.9837	0.9956	0.9980	0.9703	0.9829	0.9927	1.0059	1.0203	1.0235
	5	0.9134	0.9366	0.9493	0.9628	0.9769	0.9832	0.9333	0.9577	0.9713	0.9858	1.0010	1.0078
	10	0.9322	0.9503	0.9598	0.9696	0.9796	0.9843	0.9539	0.9729	0.9829	0.9933	1.0040	1.0089
λ_2	0	10.3117	8.9194	8.1010	7.3287	6.7064	6.4024	12.1046	10.3504	9.3940	8.5933	8.1431	7.8632
	0.5	8.3747	7.4849	6.9919	6.5473	6.2046	6.0242	9.9084	8.7781	8.2166	7.7819	7.5199	7.3028
	1	7.3529	6.7574	6.4400	6.1684	5.9675	5.8429	8.8103	8.0170	7.6411	7.3623	7.1852	7.0173
	2	6.3992	6.0889	5.9395	5.8215	5.7259	5.6464	7.6910	7.2467	7.0541	6.9209	6.8226	6.7129
	5	5.5417	5.4874	5.4677	5.4556	5.4410	5.4222	6.5254	6.4440	6.4201	6.4131	6.4077	6.3852
	10	5.2869	5.3090	5.3220	5.3362	5.3503	5.3555	6.1781	6.2076	6.2286	6.2541	6.2809	6.2897
λ_3	0	15.8455	14.2627	13.2203	11.9578	10.3905	9.5189	33.3095	28.5237	25.8911	23.6527	22.3137	21.5126
	0.5	12.0062	11.2003	10.6888	10.0767	9.3064	8.8689	28.4234	24.9643	23.2121	21.8068	20.9086	20.2493
	1	10.0770	9.7236	9.4905	9.1969	8.8026	8.5709	25.7063	23.0718	21.7861	20.7774	20.0984	19.5580
	2	8.6965	8.6428	8.5920	8.5155	8.4030	8.3357	22.7193	21.0179	20.2227	19.6138	19.1709	18.7867
	5	8.0148	8.0960	8.1331	8.1681	8.2027	8.2181	19.2706	18.6485	18.3884	18.2051	18.0462	17.8799
	10	7.9888	8.0693	8.1098	8.1505	8.1919	8.2108	17.6872	17.5547	17.5157	17.5014	17.4868	17.4500

Table 9. The first three dimensionless critical buckling loads of SS two directional FGBs with respect to gradient index and aspect ratio change.

λ	p_x	p_z											
		$L/h=5$						$L/h=20$					
		0	0.5	1	2	5	10	0	0.5	1	2	5	10
\bar{N}_{cr1}	0	49.5906	32.6756	25.3504	19.7589	16.1607	14.4341	53.3145	34.8027	26.9773	21.1935	17.8416	16.1152
	0.5	35.3718	24.7602	20.2383	16.7963	14.4031	13.0663	38.6353	26.6992	21.7735	18.1772	15.8911	14.4704
	1	26.1885	19.6987	16.9169	14.7498	13.0797	12.0455	28.6050	21.2395	18.2024	15.9510	14.3482	13.2370
	2	17.4341	14.6332	13.3924	12.3669	11.4373	10.8086	18.7056	15.6087	14.2949	13.2767	12.4178	11.7586
	5	11.3382	10.7095	10.4114	10.1341	9.8266	9.6188	11.9565	11.3058	11.0224	10.7906	10.5563	10.3641
	10	9.8204	9.6441	9.5527	9.4560	9.3367	9.2648	10.3666	10.2033	10.1327	10.0737	10.0101	9.9585
\bar{N}_{cr2}	0	160.0767	107.9494	84.0471	64.3616	49.2866	42.9415	210.1443	137.4481	106.5598	83.5726	69.9215	63.0022
	0.5	99.7755	76.0225	63.5501	52.6607	43.5556	39.2360	146.3685	102.4113	84.0710	70.4563	61.5106	56.0840
	1	67.8901	59.2406	52.3923	45.8828	39.9031	36.7749	108.2079	81.7264	70.4370	61.8009	55.5820	51.4940
	2	53.3409	46.5659	42.9634	39.5345	36.1287	34.1773	76.0689	63.2377	57.4964	52.9287	49.3324	46.7737
	5	38.8884	36.4863	35.2309	33.9732	32.5183	31.5949	52.4749	48.3128	46.4090	44.8394	43.3775	42.2166
	10	33.5665	32.6266	32.1119	31.5397	30.7894	30.3305	43.7292	42.2854	41.6358	41.0852	40.5033	40.0313
\bar{N}_{cr3}	0	264.1664	182.3956	143.0163	108.0719	78.0393	66.4945	461.4928	302.8028	234.8215	183.6713	152.1656	136.5831
	0.5	111.4783	89.1194	81.4191	74.5207	66.9518	61.2813	316.6054	223.1402	183.6237	153.7839	133.4832	121.6130
	1	76.0445	65.1351	62.6508	60.6303	58.4825	57.2290	234.6189	178.4620	154.0632	135.0305	120.9720	112.0977
	2	57.3314	56.4273	56.0330	55.6369	55.1667	54.7658	167.2355	139.3827	126.6949	116.3829	108.1004	102.4613
	5	54.7570	54.6089	54.5360	54.4559	52.9070	51.5710	117.3598	107.6882	103.1064	99.2438	95.7556	93.1277
	10	54.4277	53.4927	52.8044	51.9771	50.8003	50.0612	98.9708	95.0530	93.2189	91.6397	90.0193	88.7342

Table 10. The first three dimensionless critical buckling loads of CS two directional FGBs with respect to gradient index and aspect ratio change.

λ	p_x	P_z											
		$L/h=5$						$L/h=20$					
		0	0.5	1	2	5	10	0	0.5	1	2	5	10
\bar{N}_{cr1}	0	94.0478	62.5327	48.5623	37.5676	29.9079	26.4427	108.6714	70.9833	55.0171	43.1881	36.2764	32.7409
	0.5	64.2361	45.9588	37.8666	31.3409	26.2864	23.7234	72.7936	51.4821	42.5060	35.8030	31.4353	28.7738
	1	49.4170	37.7128	32.3767	27.9220	24.2243	22.2404	55.7821	42.1563	36.2993	31.8385	28.7177	26.6579
	2	35.9854	29.8537	26.9478	24.3867	21.9991	20.6176	40.3933	33.2910	30.1730	27.7335	25.8003	24.3857
	5	24.0509	22.2066	21.2691	20.3318	19.2618	18.6221	26.5656	24.5698	23.6820	22.9510	22.2348	21.6616
	10	19.9078	19.2916	18.9437	18.5456	18.0363	17.7548	21.9994	21.4193	21.1625	20.9435	20.7065	20.5184
\bar{N}_{cr2}	0	211.8124	144.4790	112.8046	85.7574	63.7602	54.9418	314.9555	206.2605	159.9040	125.2480	104.3546	93.8850
	0.5	136.1394	102.3665	85.4022	69.9326	56.2261	50.2907	212.0265	150.0320	123.7775	103.9845	90.7297	82.8880
	1	90.8112	78.0716	69.6881	60.6553	51.7891	47.5876	160.7081	121.9205	105.1172	92.1211	82.7459	76.7586
	2	66.2973	60.5286	56.4359	51.9724	47.2211	44.6814	115.5575	95.8646	86.9837	79.8476	74.1987	70.2817
	5	49.9960	47.3950	45.9540	44.4588	42.7184	41.6253	79.8967	73.2954	70.2218	67.6717	65.3649	63.5700
	10	43.8134	42.7397	42.1607	41.5319	40.7033	40.1608	66.7571	64.2626	63.1245	62.1625	61.1702	60.3607
\bar{N}_{cr3}	0	292.8246	204.7608	164.3272	123.8734	87.7360	74.1605	609.4937	400.6401	310.7122	242.6152	199.8402	178.9905
	0.5	144.0408	118.5416	105.9832	92.5512	76.2668	68.3449	410.6930	291.4653	240.4355	201.3645	174.2260	158.8013
	1	95.0928	85.3863	79.9084	74.5830	68.3109	64.4329	309.1080	235.6851	203.4198	177.9771	158.9640	147.2979
	2	70.4121	67.5538	66.2419	64.7182	62.6706	60.9598	221.9889	185.0573	168.0923	154.1510	142.7906	135.2306
	5	61.8920	61.4599	61.2122	60.8147	59.4126	58.1056	155.9941	143.0198	136.8016	131.4848	126.6439	123.0957
	10	60.6936	60.0134	59.4694	58.7057	57.4701	56.6617	131.9974	126.5296	123.9185	121.6305	119.2798	117.4695

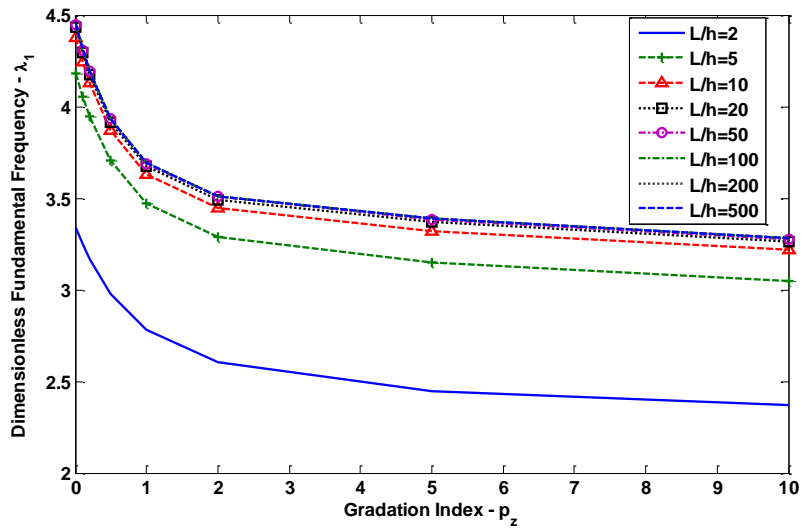
Table 11. The first three dimensionless critical buckling loads of CC two directional FGBs with respect to gradient index and aspect ratio change.

λ	p_x	P_z											
		$L/h=5$						$L/h=20$					
		0	0.5	1	2	5	10	0	0.5	1	2	5	10
\bar{N}_{cr1}	0	160.2679	108.0746	84.1405	64.4273	49.3327	42.9835	210.7416	137.8225	106.8192	83.7477	70.0605	63.1383
	0.5	105.7401	77.2659	64.0343	52.6920	43.2038	38.8848	139.4402	99.0554	81.9713	69.1074	60.5477	55.4082
	1	78.0764	61.8422	53.6846	46.2912	39.7660	36.6520	106.2280	80.8979	69.8762	61.3217	55.2183	51.3267
	2	56.5523	48.5790	44.2899	40.1780	36.3473	34.3886	78.3073	64.8021	58.6424	53.6657	49.8535	47.2692
	5	41.1913	38.0888	36.3760	34.6960	33.0948	32.1795	57.1720	51.5890	48.8771	46.5946	44.7484	43.4120
	10	35.8429	34.2305	33.3642	32.5459	31.7765	31.2651	49.7673	46.6931	45.1599	43.8403	42.7116	41.8475
\bar{N}_{cr2}	0	251.8003	173.3470	135.7595	102.7153	74.6796	63.8030	422.1958	276.9177	214.6817	167.9352	139.3281	125.1559
	0.5	140.6232	113.5445	99.1277	82.3642	65.7591	58.7161	285.3990	201.9474	166.4983	139.6432	121.4228	110.8093
	1	92.6954	81.5196	76.1113	69.4834	60.3112	55.6219	214.9611	163.3481	140.8976	123.4100	110.6102	102.5673
	2	67.2009	64.4927	62.7682	59.6803	54.9978	52.3587	153.5458	127.8516	116.1476	106.6198	99.0132	93.8715
	5	57.4832	55.0799	53.6152	52.0247	50.2484	49.2107	108.5457	99.3005	94.8022	90.9626	87.7387	85.4468
	10	52.4406	51.0256	50.2111	49.3769	48.5227	48.0110	94.6575	89.8152	87.3699	85.2529	83.5097	82.2518
\bar{N}_{cr3}	0	311.1587	219.3574	181.7947	137.2511	95.7992	80.3945	795.1563	523.8922	406.3604	316.6468	258.9558	231.3145
	0.5	146.7609	118.1641	105.9149	93.1985	78.5036	71.8940	532.5170	379.3240	313.2006	262.0044	225.6704	205.5308
	1	94.0713	84.9945	80.7869	75.1537	68.1386	65.2810	399.6407	306.1667	264.5835	231.3315	206.0308	190.9367
	2	71.8621	68.1747	65.8363	63.6533	61.9527	61.1316	288.5471	241.2640	219.1959	200.7525	185.5794	175.8422
	5	60.5675	60.1987	59.9896	59.7456	59.4106	59.1633	207.0082	189.1032	180.2318	172.4511	165.6786	161.0968
	10	59.3557	59.1538	59.0433	58.9077	58.6958	58.5202	179.3977	170.1427	165.3928	161.1602	157.5113	154.9999

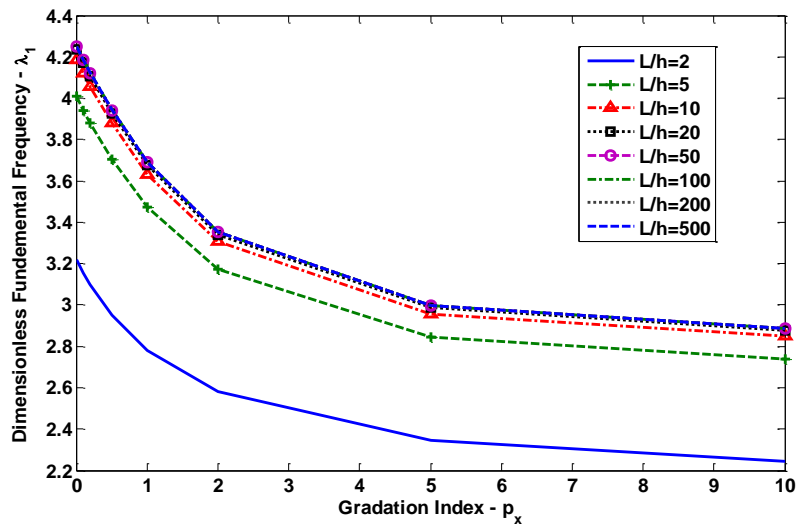
Table 12. The first three dimensionless critical buckling loads of CF two directional FGBs with respect to gradient index and aspect ratio change.

λ	p_x	p_z											
		L/h=5						L/h=20					
		0	0.5	1	2	5	10	0	0.5	1	2	5	10
\bar{N}_{cr1}	0	13.1140	8.5785	6.6516	5.2168	4.3630	3.9305	13.3996	8.7421	6.7750	5.3238	4.4887	4.0573
	0.5	7.1664	5.3152	4.5423	3.9601	3.5352	3.2533	7.2264	5.3622	4.5899	4.0166	3.6135	3.3355
	1	4.8125	3.9772	3.6173	3.3332	3.0909	2.9153	4.8322	4.0009	3.6464	3.3726	3.1490	2.9789
	2	3.3638	3.0718	2.9415	2.8324	2.7239	2.6415	3.3781	3.0908	2.9653	2.8646	2.7701	2.6933
	5	2.6302	2.5715	2.5443	2.5192	2.4901	2.4689	2.6503	2.5955	2.5718	2.5524	2.5321	2.5152
	10	2.4820	2.4663	2.4584	2.4502	2.4396	2.4325	2.5091	2.4967	2.4914	2.4871	2.4823	2.4785
\bar{N}_{cr2}	0	94.0730	63.0249	49.5540	38.6896	30.6572	26.8840	119.3550	77.9738	60.4381	47.4398	39.8306	35.9419
	0.5	64.3724	46.4348	38.5353	32.1033	26.9503	24.2522	77.6280	55.2534	45.8272	38.7754	34.1390	31.2951
	1	48.3869	37.6100	32.6207	28.4151	24.8474	22.8254	58.9276	44.9463	38.9154	34.3060	31.0667	28.9234
	2	34.8564	29.5962	27.0581	24.8284	22.7131	21.3374	42.9238	35.6744	32.4723	29.9630	27.9889	26.5381
	5	24.2830	22.6688	21.8744	21.1147	20.1978	19.5124	28.8986	26.8015	25.8675	25.1035	24.3623	23.7582
	10	20.7495	20.1574	19.8418	19.4974	19.0084	18.6401	24.1295	23.5028	23.2275	22.9963	22.7482	22.5449
\bar{N}_{cr3}	0	150.0995	103.2808	84.9106	68.5902	52.1077	43.9219	324.8583	212.7835	164.9817	129.2274	107.6292	96.8097
	0.5	122.3114	88.5317	74.3293	61.6366	48.7523	41.9566	216.1440	153.3609	126.7567	106.6771	93.1813	85.1794
	1	88.9437	73.6067	64.8398	56.1002	46.4543	40.7481	163.3633	124.4023	107.4885	94.3903	84.9201	78.8548
	2	65.5538	59.1107	54.7532	49.9332	43.7311	39.3138	117.9672	98.1425	89.1910	81.9929	76.2784	72.3031
	5	50.7442	47.7075	45.8941	43.8063	40.4773	37.4451	82.2164	75.4954	72.3590	69.7490	67.3747	65.5315
	10	44.6512	43.1330	42.1785	40.9497	38.5491	36.1142	68.9235	66.3589	65.1825	64.1807	63.1358	62.2878

The first three dimensionless critical buckling loads of the 2D-FGBs are revealed in Tables 9-12. It is clear that the first three critical buckling loads decrease for all type of end conditions as the gradient indexes increase. It is interesting that the shear deformation effect becomes significantly important as the buckling mode number increases. For all types of BCs, the relative difference between critical buckling loads with respect to variation of the aspect ratio increases as the buckling mode increases. The first dimensionless critical buckling loads of the 2D-FG CC beam with $p_z=1$ and $p_x=1$ are $\bar{N}_{cr1} = 53.6846$ and $\bar{N}_{cr1} = 69.8762$ for $L/h=5$ and $L/h=20$, respectively. On the other hand, the third dimensionless critical buckling loads are $\bar{N}_{cr3} = 80.7869$ and $\bar{N}_{cr3} = 264.5835$ for $L/h=5$ and $L/h=20$, respectively. Using the value of the aspect ratio $L/h=5$ as a reference, the relative differences are % 30 and % 228 for CC beams with $L/h=5$ and $L/h=20$, respectively. For SS beams, the values are % 8 and % 153 for $L/h=5$ and $L/h=20$, respectively. The relative differences are % 35 and % 202 for CS beams with $L/h=5$ and $L/h=20$, respectively. And finally, for CF beams, they are % 3 and % 107 for $L/h=5$ and $L/h=20$, respectively. These results can be compared with ones given in [35]. It is clear that the relative difference is the least for CF beam while it is the most for CC beam.



a) $p_x = 1$



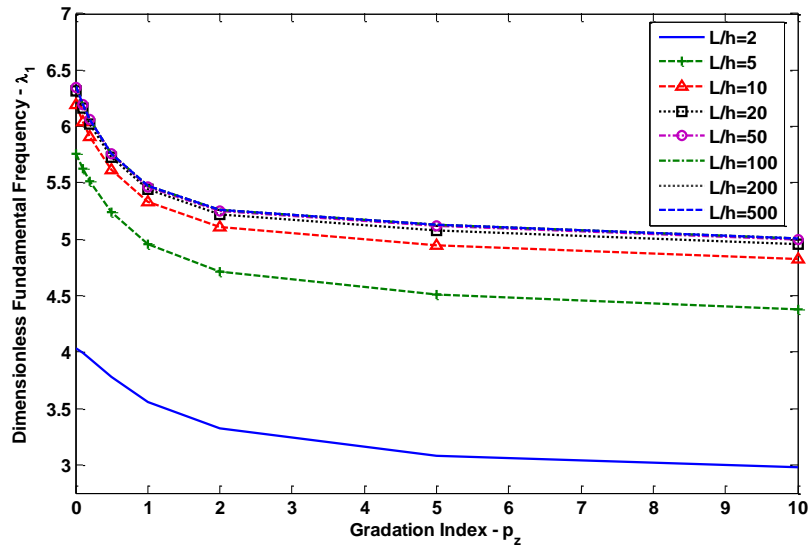
b) $p_z = 1$

Figure 2. Variation of the dimensionless fundamental frequencies of SS two directional FGBs with respect to variation of gradient indexes and aspect ratios a) $p_x = 1$ and b) $p_z = 1$

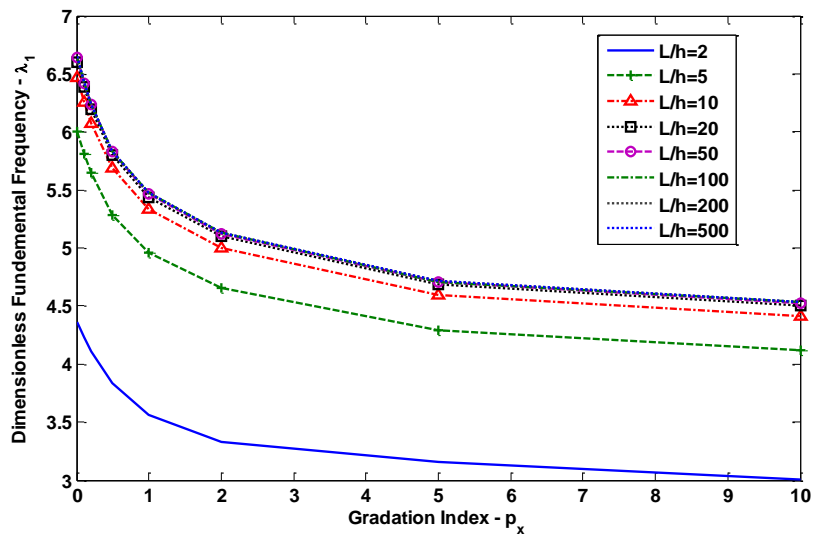
Figures 2 to 5 are plotted to illustrate the effect of gradient indexes, p_x and p_z , and aspect ratios on the dimensionless fundamental frequencies of the 2D-FGBs for all type of boundary conditions. It is observed that with the increase of the gradient indexes the dimensionless fundamental frequencies decrease because of decreasing the rigidity of the beam for SS, CS and CC beams. When the gradient index in the z direction is set to 1, the dimensionless fundamental frequencies decrease with respect to variation of the gradient index in the x direction for all aspect ratios. Moreover, as the gradient index in the x direction is set to 1, the dimensionless fundamental frequencies of CF 2D-FGBs decrease for the aspect ratio $L/h \leq 5$. For higher values of aspect ratio of CF 2D-FGBs with $p_x = 1$ and $1 \leq p_z \leq 5$, the dimensionless fundamental frequencies increase. On the other hand, for CF 2D-FGBs with $L/h \geq 10$, $p_x = 1$ and $5 < p_z \leq 10$, the dimensionless fundamental frequencies decrease. As it is explained before, the vibration behavior of the 2D-FGBs with CF boundary condition is significantly

affected with the variation of the mass and Young’s modulus which depend on the gradient index in the x direction, mode numbers and aspect ratios.

It is found that the reduction in the dimensionless fundamental frequencies because of the gradient index variation in the x direction is more than the gradient index variation in the z direction for all boundary conditions and aspect ratios. According to the presented 2D- FGBs in Figures 2 to 5, the numerical results show that a thick 2D- FG beam can be defined with the aspect ratio $L/h \leq 10$ for the free vibration analysis except the CF beam with $p_z = 1$ and $0 < p_x \leq 10$.

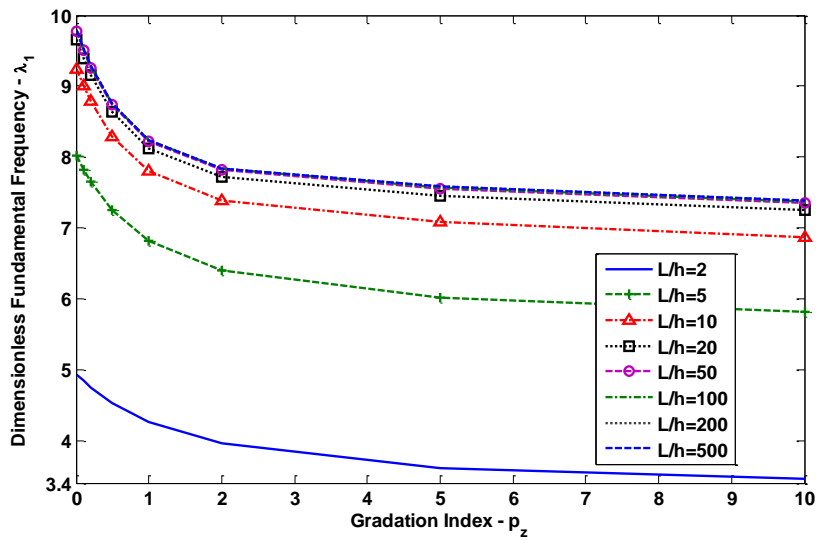


a) $p_x = 1$

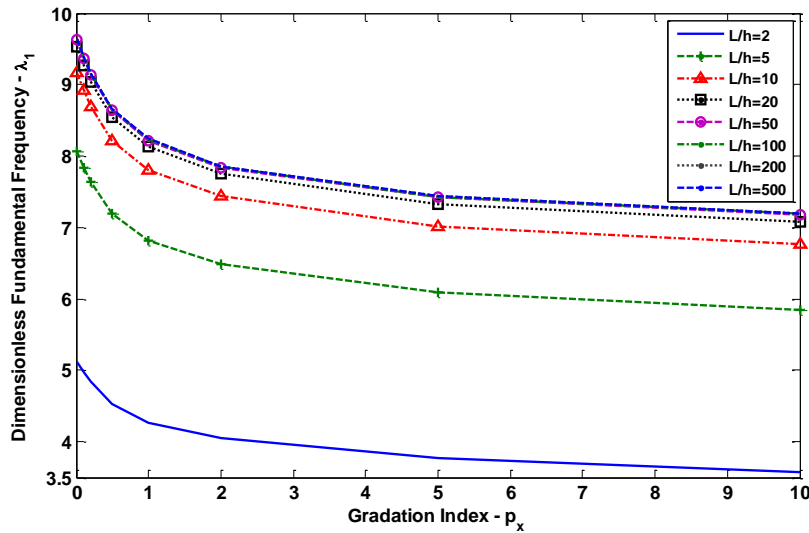


b) $p_z = 1$

Figure 3. Variation of the dimensionless fundamental frequencies of CS two directional FGBs with respect to variation of gradient indexes and aspect ratios a) $p_x = 1$ and b) $p_z = 1$



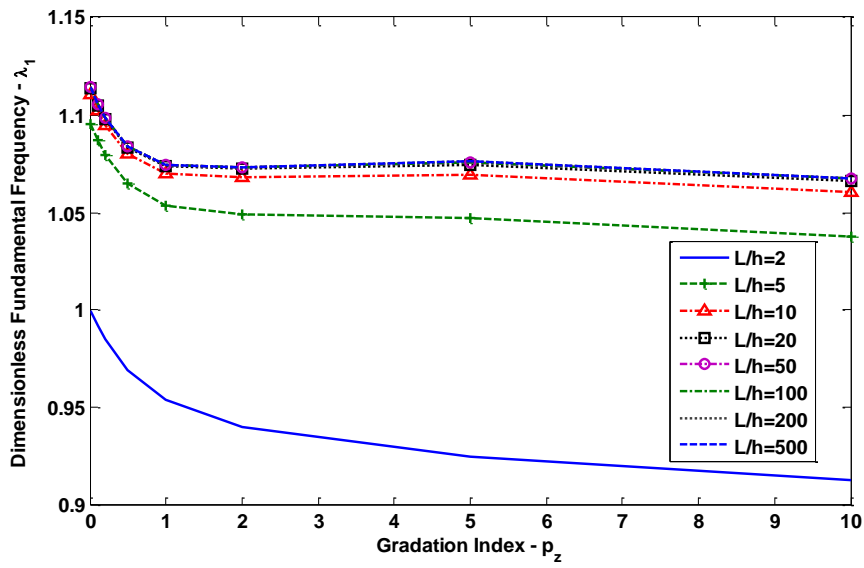
a) $p_x = 1$



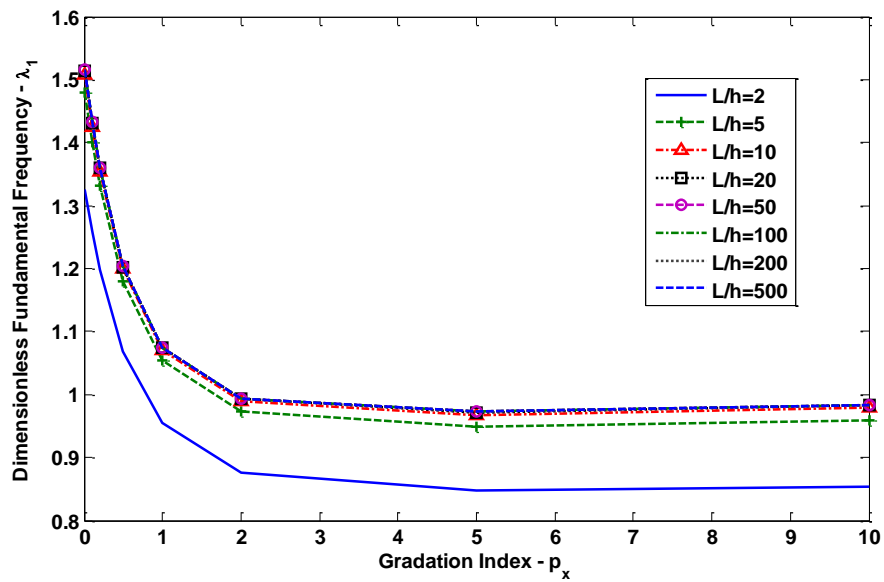
b) $p_z = 1$

Figure 4. Variation of the dimensionless fundamental frequencies of CC two directional FGBs with respect to variation of gradient indexes and aspect ratios a) $p_x = 1$ and b) $p_z = 1$

Figures 6 to 9 examine the effect of the gradient indexes, aspect ratios and boundary conditions on the first critical buckling loads of the 2D-FGBs. As expected, as the aspect ratio increases, the dimensionless first critical buckling load increases for all types of BCs and the values of the gradient indexes studied in these examples. Besides, the dimensionless first critical buckling load decreases while the gradient index increases in any direction. It is clear that the highest first critical buckling loads are seen in CC beams followed by CS, SS and CF beams. It is also observed that the reduction in the dimensionless first critical buckling loads because of the gradient index variation in the x direction is more than the gradient index variation in the z direction for all boundary conditions and aspect ratios. Moreover, with the increase of the aspect ratio, the critical buckling loads become very close to each other after in the region, for SS and CS $L/h \geq 20$, CF $L/h \geq 10$ and CC $L/h \geq 30$. On the other hand, for CC beams, the effect of the shear deformation is significant in the region $L/h \leq 15$.

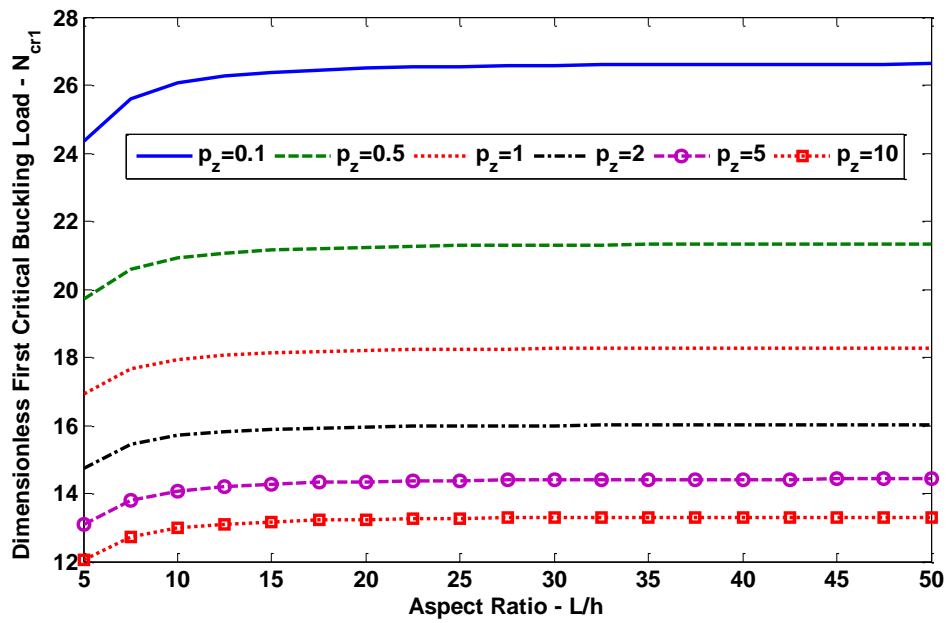


a) $p_x = 1$

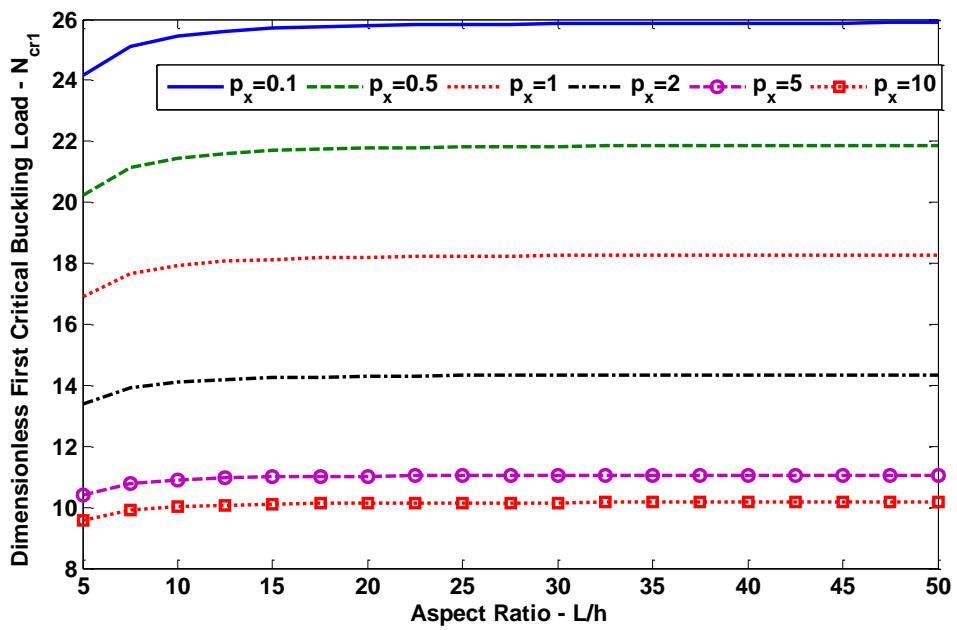


b) $p_z = 1$

Figure 5. Variation of the dimensionless fundamental frequencies of CF two directional FGBs with respect to variation of gradation indexes and aspect ratios a) $p_x = 1$ and b) $p_z = 1$



a) $p_x = 1$



b) $p_z = 1$

Figure 6. Variation of the dimensionless first critical buckling loads of SS two directional FGBs with respect to variation of gradient indexes and aspect ratios a) $p_x = 1$ and b) $p_z = 1$

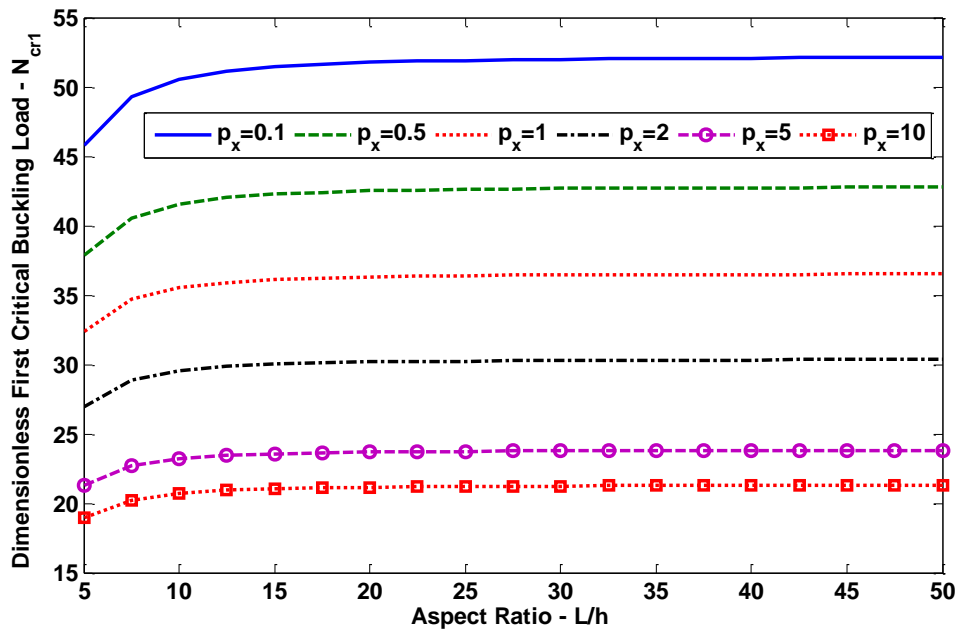
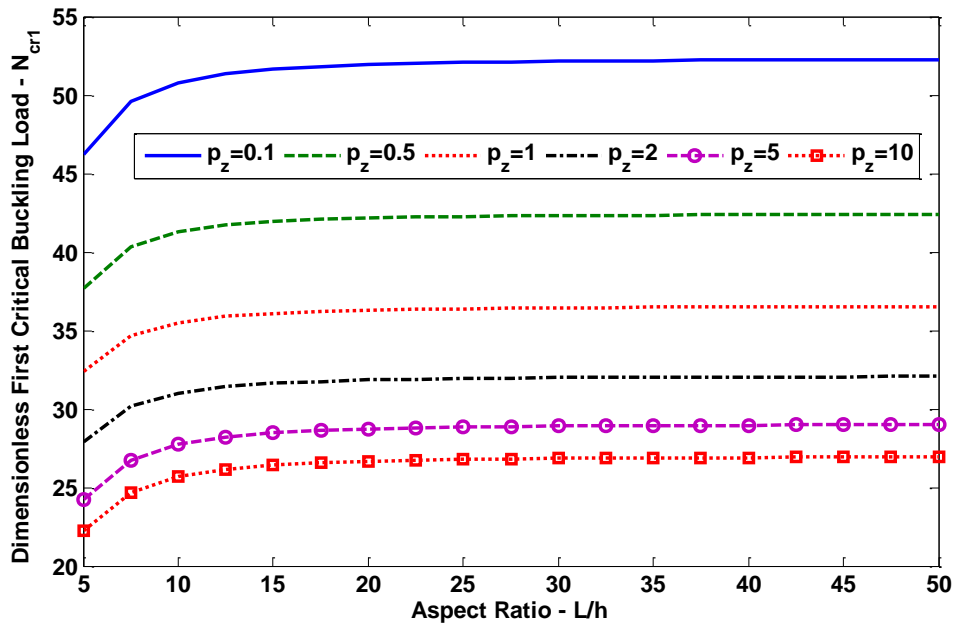


Figure 7. Variation of the dimensionless first critical buckling loads of CS two directional FGBs with respect to variation of gradient indexes and aspect ratios a) $p_x = 1$ and b) $p_z = 1$

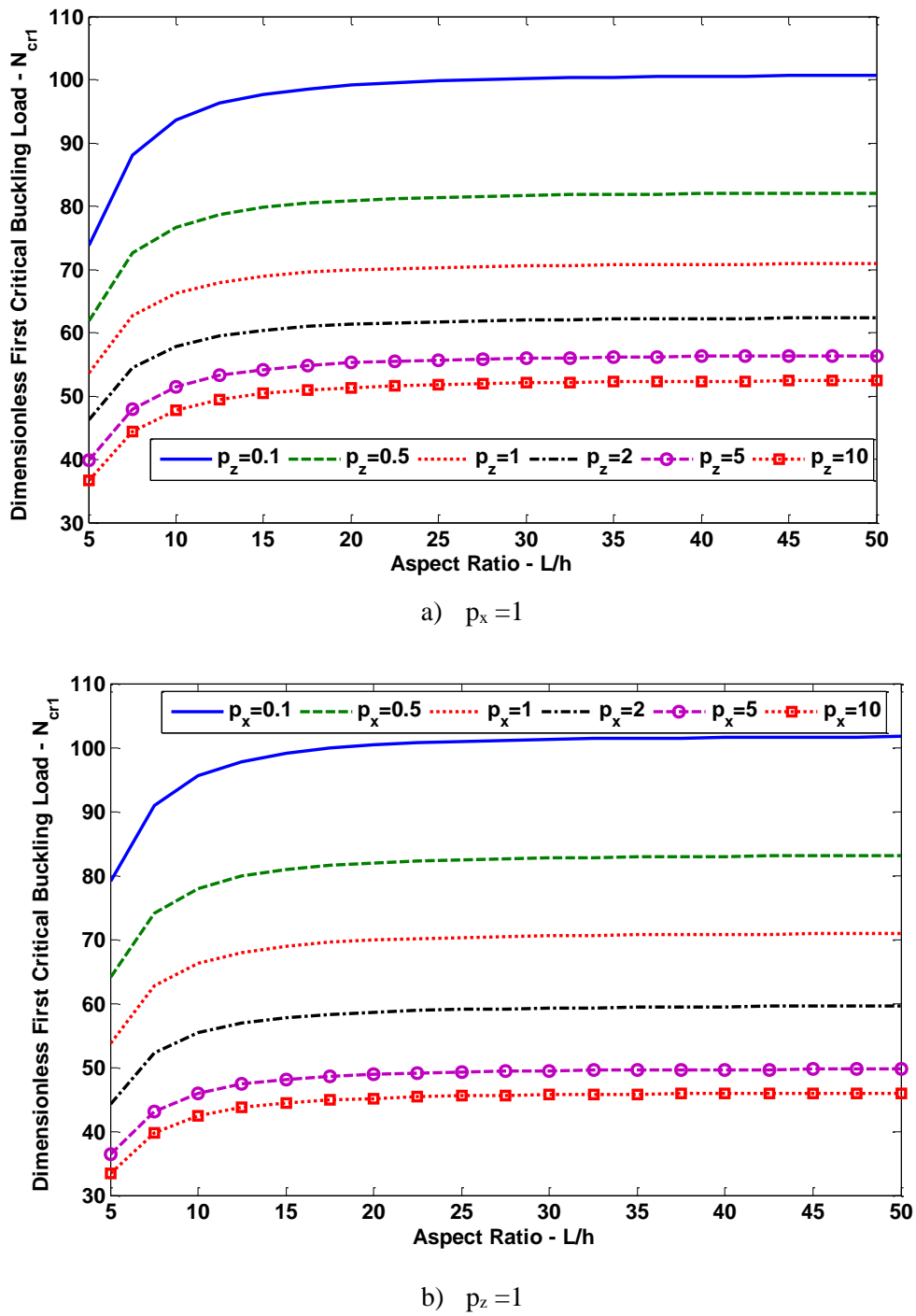
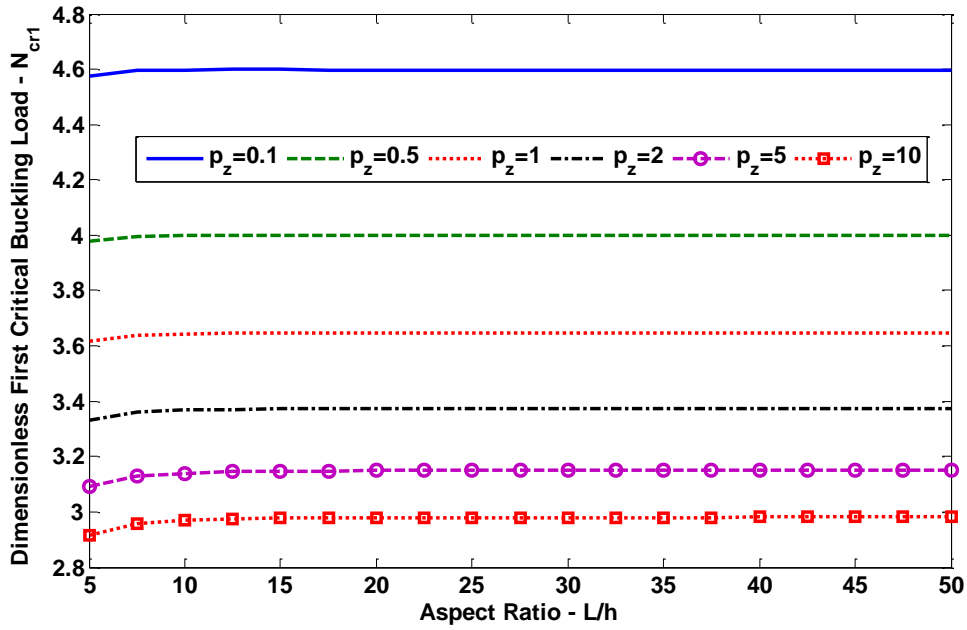
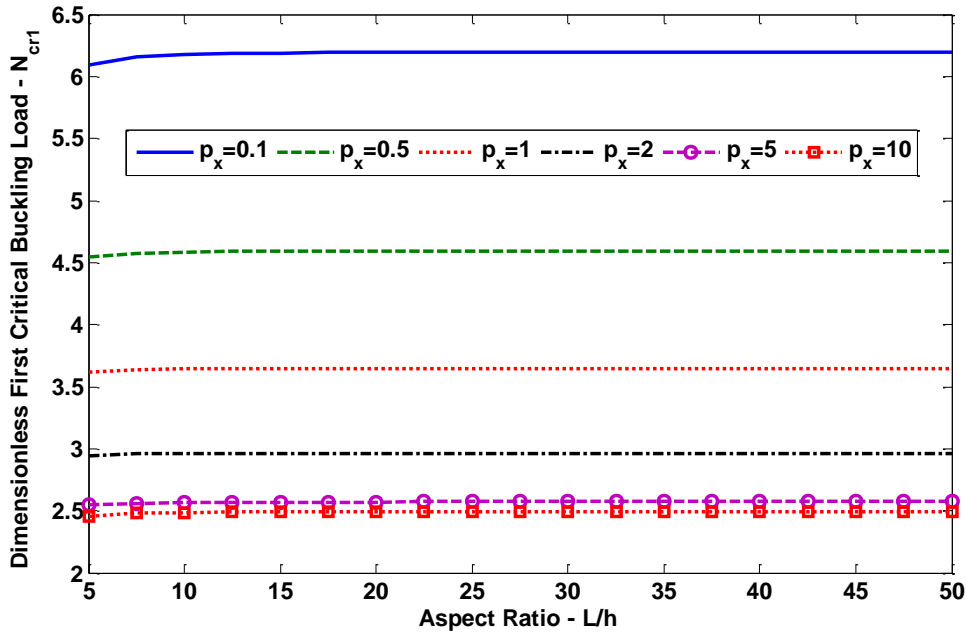


Figure 8. Variation of the dimensionless first critical buckling loads of CC two directional FGBs with respect to variation of gradient indexes and aspect ratios a) $p_x = 1$ and b) $p_z = 1$



a) $p_x = 1$



b) $p_z = 1$

Figure 9. Variation of the dimensionless first critical buckling loads of CF two directional FGBs with respect to variation of gradient indexes and aspect ratios a) $p_x = 1$ and b) $p_z = 1$

The first four normalized vibration mode shapes of SS, CS, CC and CF 2D-FGBs with the gradient indexes, $p_z = 1$ and $p_x = 1$, are illustrated in Figures 10 to 13. Actually, the obtained mode shape is a quadruple mode shape. Since the small stretching deformation occurs, the resulting mode shape is referred as triply coupled mode, which is substantial involving axial, shear and bending deformations for all types of end conditions. The first four flexural normalized buckling mode shapes of the two directional FGBs for all type of boundary conditions are presented in Figure 14 ($L/h=5$, $p_z=1$ and $p_x=1$). One may expect that for a homogeneous CC beam the mode shapes are symmetric about the

midpoint of the beam. However, because of the material variation along the length of the beam the mode shapes become anti-symmetric about the midpoint of the 2D-FGB.

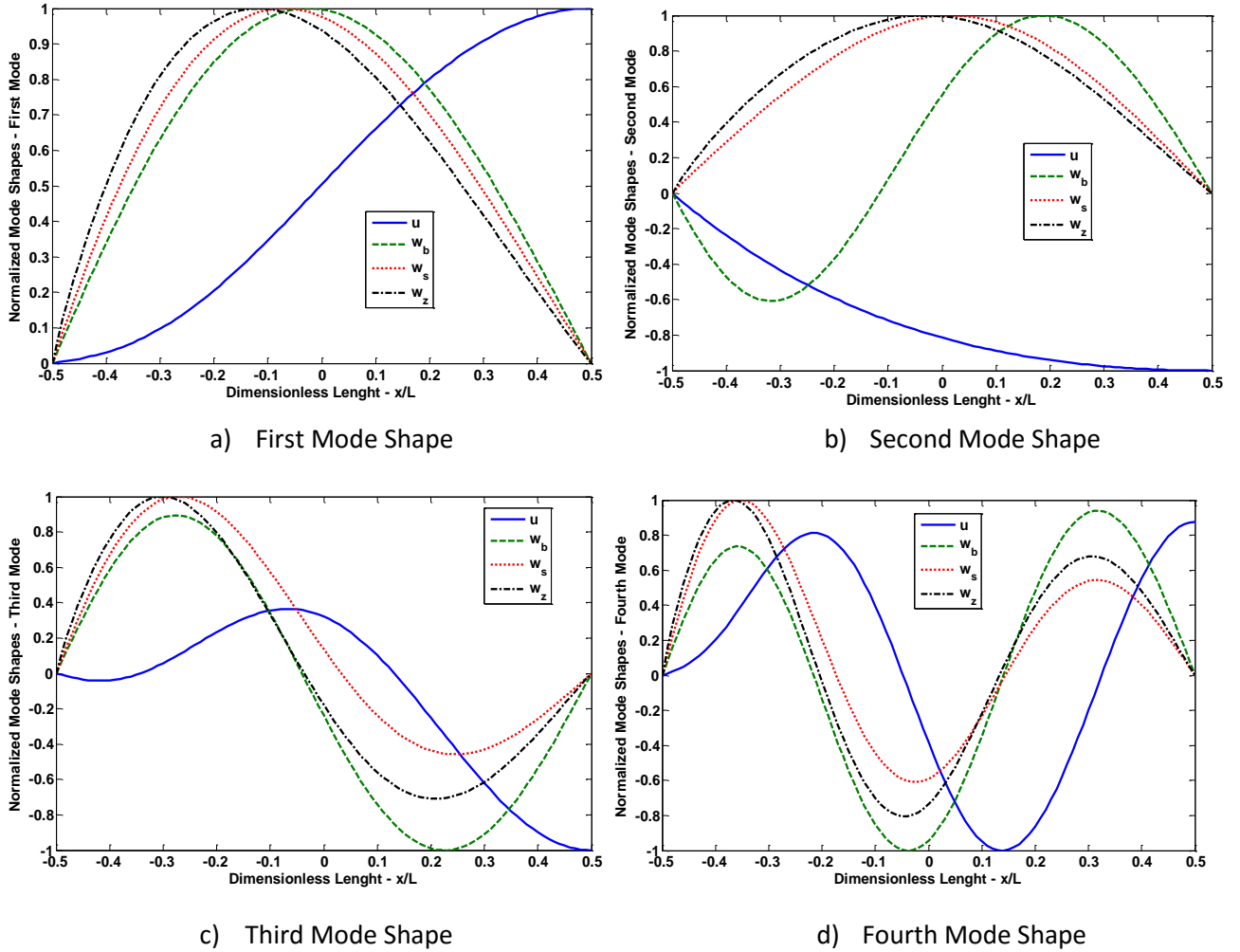
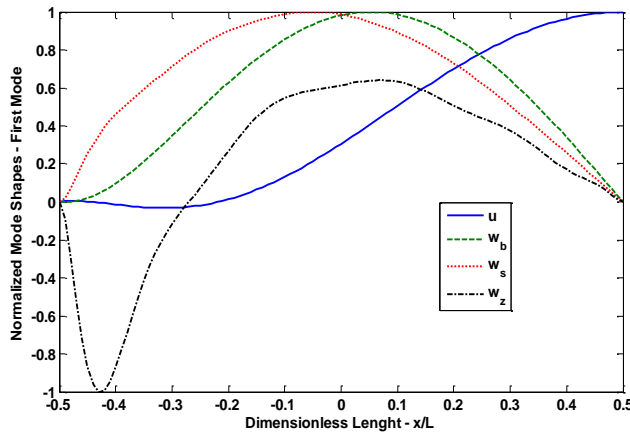
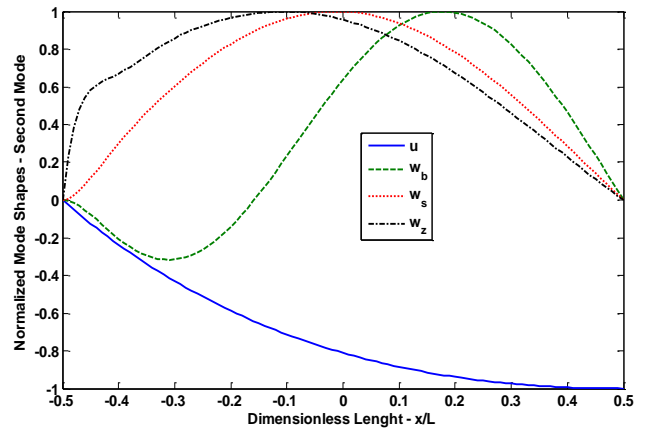


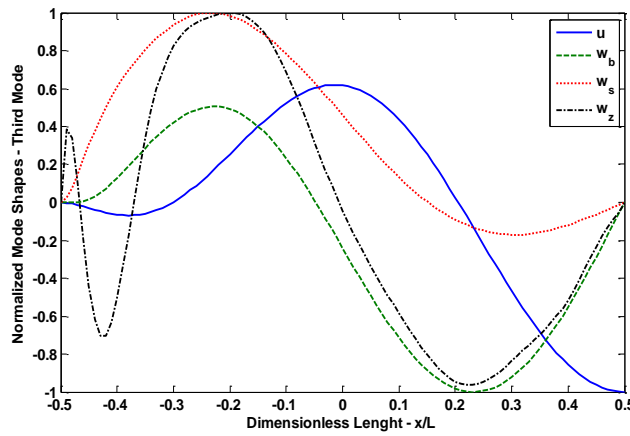
Figure 10. First four normalized vibration mode shapes of SS two directional FGBs ($L/h=5$, $p_x=1$ and $p_z=1$)



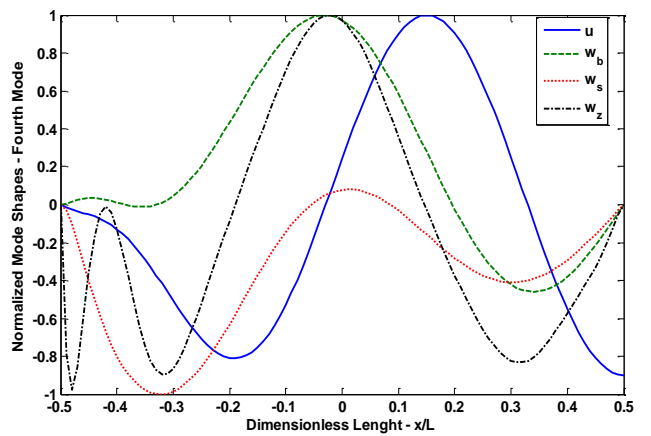
a) First Mode Shape



b) Second Mode Shape



c) Third Mode Shape



d) Fourth Mode Shape

Figure 11. First four normalized vibration mode shapes of CS two directional FGBs ($L/h=5$, $p_x=1$ and $p_z=1$)

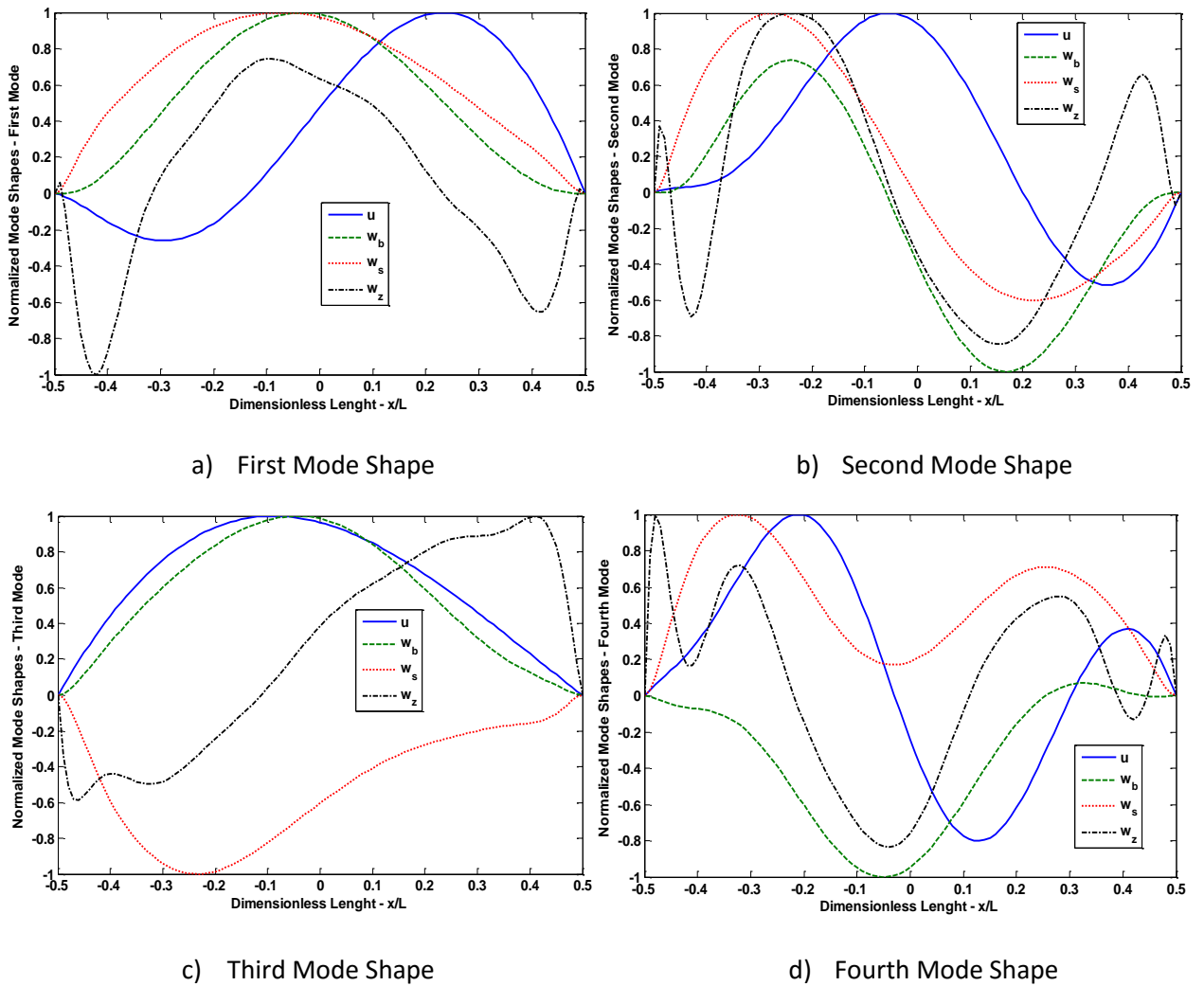
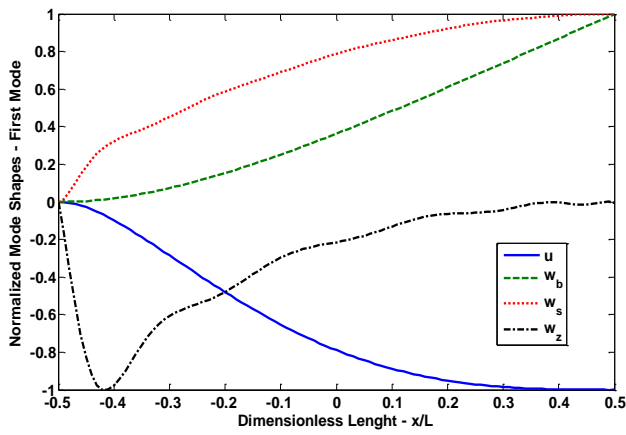
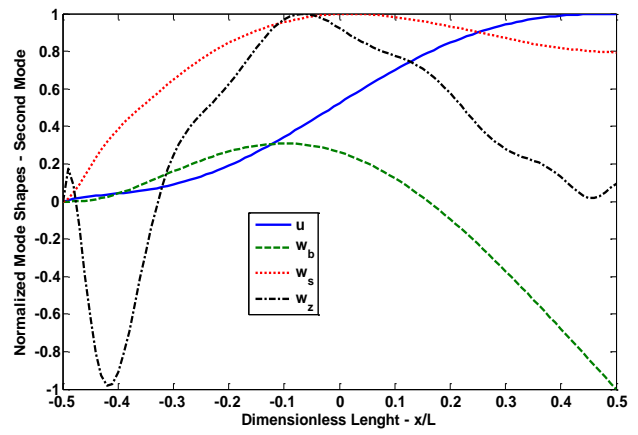


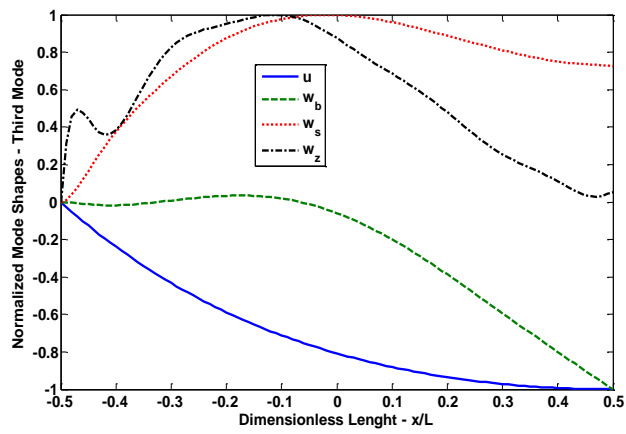
Figure 12. First four normalized vibration mode shapes of CC two directional FGBs ($L/h=5$, $p_x=1$ and $p_z=1$)



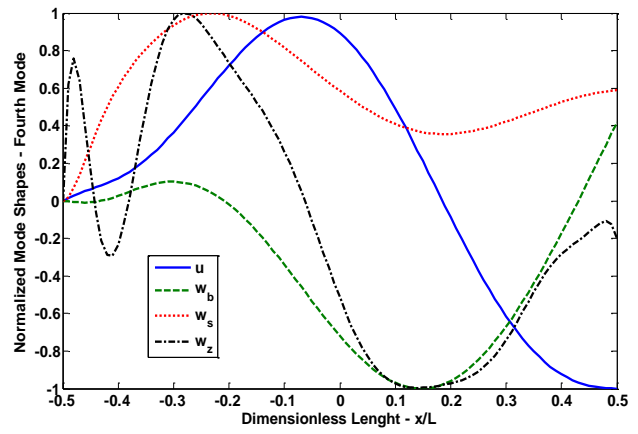
a) First Mode Shape



b) Second Mode Shape



c) Third Mode Shape



d) Fourth Mode Shape

Figure 13. First four normalized vibration mode shapes of CF two directional FGBs ($L/h=5$, $p_x=1$ and $p_z=1$)

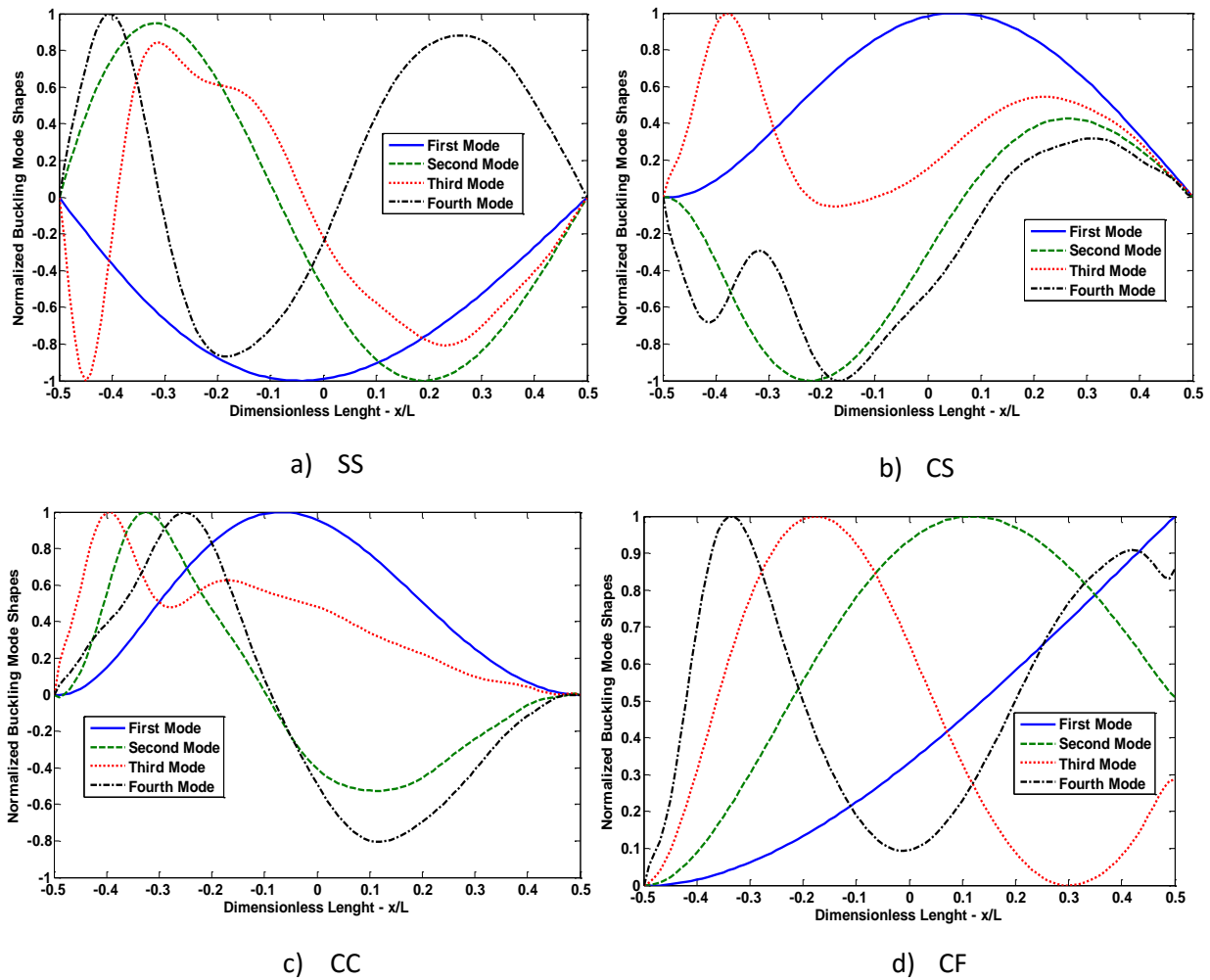


Figure 14. First four flexural (\bar{W}) normalized buckling mode shapes of two directional FGBs for various boundary conditions ($L/h=5$, $p_x=1$ and $p_z=1$)

4. CONCLUSION

In this paper, the free vibration and buckling behaviors of the two directional functionally graded beams having different boundary conditions are investigated by employing a four-unknown shear and normal deformation theory. The governing equations of motions are obtained via Lagrange equations in conjunction with polynomials added auxiliary functions that satisfy the boundary conditions. Analytical polynomial displacement solutions are derived for Simply supported – Simply supported (SS), Clamped-Simply supported (CS), Clamped – clamped (CC) and Clamped-free (CF) boundary conditions by employing various gradient indexes in both axial and thickness directions. The computed results in terms of dimensionless frequencies and critical buckling loads are compared with the results from previous studies. It is found that computed results show excellent agreement with previous ones. The effects of the boundary conditions, gradient indexes and aspect ratios on the dimensionless frequencies and critical buckling loads of the 2D-FGBs are discussed. Based on the extensive analysis, the main important results are given below:

- The dimensionless frequencies and buckling loads of the 2D-FGBs are greatly affected by the gradient indexes. However, the effect of the gradient index in the x direction is more significant than the gradient index in the z direction.

- Increment of the gradient indexes, the dimensionless fundamental frequencies decrease because of decreasing the rigidity of the beam for SS, CS and CC beams.
- The effect of the mass on the dimensionless frequencies of the SS, CS and CC 2D-FGBs is a bit more dominant than the effect of the Young's modulus. The vibration behavior of the 2D-FGBs with CF boundary condition is significantly affected with the variation of the mass and Young's modulus. This effect mainly depends on the gradient index value in the x direction, mode number and aspect ratio.
- The highest free vibration frequencies for 2D-FGBs are obtained while the CC boundary condition is employed. The lowest frequencies are observed for CF beams followed by SS and CS beams.
- Increment of the gradient indexes, the critical buckling load increase.
- The shear deformation effect becomes important as the buckling mode number increases. For all types of BCs, the relative difference between critical buckling loads increases as the buckling mode increases.
- As the aspect ratio increases, the shear deformation effect on the critical buckling loads of the 2D-FGBs decreases. It is observed that CC 2D-FGB is much more sensitive to shear deformation effect than the other 2D-FGB models.
- A triply coupled mode shape which is substantial involving axial, shear and bending deformations for all types of end conditions is obtained.
- The highest first critical buckling loads are seen in CC beams followed by CS, SS and CF beams.
- To meet the design requirements, the vibration and buckling behaviors of the 2D-FGBs can be controlled by selecting suitable gradient indexes.
- Especially for thick beams, the shear deformation effect is very important and the proposed theory provides accurate results and is efficient in solving the vibration and buckling behaviors of the 2D-FGBs.

REFERENCES

- [1] Chakraborty A., Gopalakrishnan S, Reddy JN. A new beam finite element for the analysis of functionally graded materials. *Int J Mech Sci.* 2003; 45(3) 519–539.
- [2] Li X.F. A unified approach for analyzing static and dynamic behaviors of functionally graded Timoshenko and Euler–Bernoulli beams. *J Sound Vib.* 2008; 318 (4–5) 1210–1229.
- [3] Li SR., Batra R.C. Relations between buckling loads of functionally graded Timoshenko and homogeneous Euler–Bernoulli beams. *Compos Struct.* 2013; 95 5–9.
- [4] Nguyen TK., Vo TP., Thai H.T. Static and free vibration of axially loaded functionally graded beams based on the first-order shear deformation theory. *Composites B.* 2013; 55 147–57.
- [5] Pradhan K, Chakraverty S. Free vibration of euler and Timoshenko functionally graded beams by Rayleigh–Ritz method. *Composites B.* 2013; 51 175–84.

- [6] Sina S, Navazi H, Haddadpour H. An analytical method for free vibration analysis of functionally graded beams, *Mater Des.* 2009; 30(3) 741–7.
- [7] Aydogdu M, Taskin V. Free vibration analysis of functionally graded beams with simply supported edges. *Mater Des.* 2007; 28 1651–1656.
- [8] Kapuria S, Bhattacharyya, M, Kumar, AN. Bending and free vibration response of layered functionally graded beams A theoretical model and its experimental validation. *Compos Struct.* 2008; 82(3) 390–402.
- [9] Kadoli R., Akhtar K., Ganesan N. Static analysis of functionally graded beams using higher order shear deformation theory. *Appl Math Model.* 2008; 32 (12): 2509–2525.
- [10] Benatta MA, Mechab I, Tounsi, A., Bedia, E.A.A. Static analysis of functionally graded short beams including warping and shear deformation effects. *Comput Mater Sci.* 2008; 44(2): 765–773.
- [11] Ben-Oumrane S, Abedlouahed T., Ismail M., Mohamed, B.B., Mustapha, M., Abbas, A.B.E.. A theoretical analysis of flexional bending of Al/Al₂O₃ S-FGM thick beams. *Comput Mater Sci.* 2009; 44(4): 1344–1350.
- [12] Li XF, Wang BL, Han JC. A higher-order theory for static and dynamic analyses of functionally graded beams. *Arch Appl Mech.* 2010; 80: 1197–1212.
- [13] Zenkour AM., Allam MNM, Sobhy M. Bending analysis of fg viscoelastic sandwich beams with elastic cores resting on Pasternaks elastic foundations. *Acta Mech.* 2010; 212: 233–252.
- [14] Simsek M. Fundamental frequency analysis of functionally graded beams by using different higher-order beam theories. *Nucl Eng Des.* 2010; 240(4): 697–705.
- [15] Thai HT, Vo TP. Bending and free vibration of functionally graded beams using various higher-order shear deformation beam theories. *Int J Mech Sci.* 2012; 62 (1): 57–66.
- [16] Vo TP, Thai HT, Nguyen TK, Inam F. Static and vibration analysis of functionally graded beams using refined shear deformation theory. *Meccanica.* 2014; 49(1): 155–68.
- [17] Vo TP, Thai HT, Nguyen TK, Maheri A, Lee J. Finite element model for vibration and buckling of functionally graded sandwich beams based on a refined shear deformation theory. *Eng Struct.* 2014; 64: 12–22.
- [18] Nguyen TK, Nguyen TTP, Vo TP, Thai HT. Vibration and buckling analysis of functionally graded sandwich beams by a new higher-order shear deformation theory. *Composites B.* 2015; 76: 273–85.
- [19] Nguyen TK, Nguyen BD. A new higher-order shear deformation theory for static, buckling and free vibration analysis of functionally graded sandwich beams. *J Sandwich Struct Mater.* 2015; 17(6): 613–31.
- [20] Carrera E, Giunta G, Petrolo M. *Beam structures classical and advanced theories.* John Wiley & Sons; 2011.

- [21] Giunta G, Belouettar S, Carrera E. Analysis of FGM beams by means of classical and advanced theories. *Mech Adv Mater Struct.* 2010; 17(8): 622–35.
- [22] Mashat DS., Carrera E, Zenkour AM, Khateeb, S.A.A., Filippi, M. Free vibration of FGM layered beams by various theories and finite elements. *Composites B.* 2014; 59: 269–78.
- [23] Filippi M., Carrera, E., Zenkour A.M. Static analysis of FGM beams by various theories and finite elements. *Composites B.* 2015; 72: 1–9.
- [24] Vo, T.P., Thai H.T., Nguyen T.K., Inam, F., Lee, J. A quasi-3D theory for vibration and buckling of functionally graded sandwich beams. *Compos Struct.* 2015; 119: 1–12.
- [25] Vo T.P., Thai, H.T., Nguyen T.K., Inam, F., Lee, J. Static behaviour of functionally graded sandwich beams using a quasi-3D theory, *Composites B.* 2015; 68: 59–74.
- [26] Mantari J.L., Yarasca J. A simple and accurate generalized shear deformation theory for beams, *Compos Struct.* 2015; 134: 593–601.
- [27] Mantari, J.L. A refined theory with stretching effect for the dynamics analysis of advanced composites on elastic foundation. *Mech Mater.* 2015; 86: 31–43.
- [28] Mantari J.L. Refined and generalized hybrid type quasi-3D shear deformation theory for the bending analysis of functionally graded shells, *Composites B.* 2015; 83: 142–52.
- [29] Nguyen T.K., Vo T.P., Nguyen B.D., Lee J. An analytical solution for buckling and vibration analysis of functionally graded sandwich beams using a quasi-3D shear deformation theory. *Compos. Struct.* 2016; 156: 238-252.
- [30] A. Frikha, A. Hajlaoui, M. Wali, F. Dammak. A new higher order C0 mixed beam element for FGM beams analysis, *Composites B.* 2016; 106: 181-9.
- [31] Nemat-Alla M. Reduction of thermal stresses by developing two-dimensional functionally graded materials. *Int. Journal of Solids and Structures.* 2003; 40: 7339–7356.
- [32] Goupee A.J., Vel S.S. Optimization of natural frequencies of bidirectional functionally graded beams. *Struct. Multidisc. Optim.* 2006; 32: 473–484.
- [33] Lü C.F., Chen W.Q., Xu R.Q., Lim C.W. Semi-analytical elasticity solutions for bidirectional functionally graded beams. *Int. Journal of Solids and Structures.* 2008; 45: 258–275.
- [34] Zhao L., Chen W.Q., Lü C.F. Symplectic elasticity for two-directional functionally graded materials. *Mech. Mater.* 2012; 54: 32–42.
- [35] Simsek M. Bi-Directional functionally graded materials (BDFGMs) for free and forced vibration of Timoshenko beams with various boundary conditions. *Compos. Struct.* 2015; 141: 968–978.
- [36] Simsek M. Buckling of Timoshenko beams composed of two-dimensional functionally graded material (2D-FGM) having different boundary conditions. *Compos. Struct.* 2016; 149: 304–314.
- [37] Karamanli A. Elastostatic analysis of two-directional functionally graded beams using various beam theories and Symmetric Smoothed Particle Hydrodynamics method. *Compos. Struct.* 2017; 160: 653-669.

- [38] Nazargah M. Fully coupled thermo-mechanical analysis of bi-directional FGM beams using NURBS isogeometric finite element approach. *Aerospace Science and Technology*. 2015; 45: 154-164.
- [39] Pydah A., Batra R.C. Shear deformation theory using logarithmic function for thick circular beams and analytical solution for bi-directional functionally graded circular beams. *Compos. Struct.* 2017; 172: 45-60.
- [40] Karamanli A. Bending behaviour of two directional functionally graded sandwich beams by using a quasi-3d shear deformation theory. *Compos. Struct.* 2017; 174: 70-86.
- [41] Zafarmand H., Hassani B. Analysis of two-dimensional functionally graded rotating thick disks with variable thickness. *Act Mech.* 2014; 225: 453-464.
- [42] Nguyen D.K., Nguyen Q.H., Tran T.T., Bui V.T. Vibration of bi-dimensional functionally graded Timoshenko beams excited by a moving load. *Act Mech.* 2017; 228: 141-155.
- [43] Hacıyev V.C., Sofiyev A.H., Kuruoğlu V.T. Free bending vibration analysis of thin bidirectionally exponentially graded orthotropic rectangular plates resting on two-parameter elastic foundations. *Compos. Struct.* 2018; 184: 372-377.